Programa de Estudios de Honor
Universidad de Puerto Rico
Recinto de Río Piedras

Honors Program
University of Puerto Rico
Rio Piedras Campus

TESIS O PROYECTO DE CREACIÓN

APROBADO COMO REQUISITO PARCIAL DEL
PROGRAMA DE ESTUDIOS DE HONOR

COMITÉ DE TESIS O PROYECTO DE CREACIÓN	NOMBRE
Mentor	Marvin J. Bayro, Ph.D.
Director de Estudios	José A. Rodríguez Martínez, Ph.D.
Lector	Juan S. Ramírez, Ph.D
Lector	Esther Peterson, Ph.D.
Lector	_____

Visto Bueno: Dra. Ana C. Guzzi Vasques
Directora Asociada PREH

25 de mayo de 2022
Fecha

University of Puerto Rico

Río Piedras Campus

Honors Program

Optimization of Cardiolipin Nanoparticle Assembly for Cytochrome c Encapsulation

Gabrielys Encarnación López

Committee:

Dr. Marvin Bayro

Dr. Juan Ramírez

Dr. Esther Peterson

Dr. José Rodríguez

Abstract

Lipid nanoparticles and their ability to transport drugs into the cell cytosol without being detected by the immune system can play a meaningful role in inducing apoptosis in cancer cells. The application of lipid nanoparticles such as the complex of cytochrome c (Cytc) and cardiolipin (CL) to induce apoptosis in cancer cells has been explored in recent years as a novel therapy for this illness. However, detailed structure of this nanoparticle complex and the molecular basis for its formation remain elusive. To understand and optimize the formation of Cytc-CL nanoparticles, we propose to analyze the assembly of the Cytc-CL complex under different CL compositions and in the presence of other naturally occurring lipids. In this study we use dynamic light scattering (DLS), scanning electron microscopy (SEM), nuclear magnetic resonance (NMR), UV-Vis spectroscopy, and fluorescence spectrophotometry to elucidate which formulation has more homogenous assembly of protein-lipid conjugates.

Project Aim

Lipid nanoparticles (LNPs) are promising drug delivery systems due to their ability to transport hydrophilic and hydrophobic molecules through the cell membrane and into the cytosol.[1] These nanoparticles can be manufactured in a laboratory and be used to treat many illnesses, including different types of cancer.[2] Female breast cancer is the most common cancer diagnosed worldwide, having surpassed lung cancer as the leading cause of global cancer incidence.[3] Most anticancer therapies induce apoptosis, also known as cell suicide or programmed cell death. Although current treatments have good success rates, they often have high toxicity and may affect adjacent healthy cell tissue .[4] LNPs, on the other hand, present lower toxicity and targeting specificity, which makes them a promising method to treat breast cancer. However, the mechanism followed by these nanoparticles to induce apoptosis and their optimal structure remains unknown. In the development of potentially therapeutic LNPs, structural homogeneity is a matter of utmost importance and often a prerequisite for further functionalization.

To search for conditions that favor high structural homogeneity, we will prepare a LNP composed of Cytc and different molar excesses of CL, which has proven to play a crucial role in the execution of cell death, taking advantage of the natural physical and chemical properties of these molecules.[5] We will also prepare nanoparticle formulations of Cytc with neutral or positively charged lipids, as well as formulations that combine CL with these other lipids, to uncover ideal conditions for the preparation of Cytc-CL nanoparticles. Specifically, we aim to:

Aim: Optimize the production of Cytc-CL nanoparticles based on structural analysis

Hypothesis: The electrostatic interactions that guide native protein-lipid association will lead to the homogeneous assembly of protein- lipid liposomes.

We will prepare different nanoparticle formulations of Cytc with the following lipids: (a) CL, (b) phosphatidylcholine (PC), and (c) phosphatidylethanolamine (PE) using different molar concentrations of these lipids. Particle size and polydispersity index (PDI) will be measured using a Dynamic Light Scattering (DLS) analysis to determine if we have a homogenous solution. We expect small sized nanoparticles, so they can make it through the cell membrane, with a PDI value of 0.30 or less, characteristic for homogenous nanoparticles. We also expect to see complete coverage of Cytc molecules by the lipids. The nanoparticles will be analyzed using Scanning Electron Microscopy (SEM), liquid-state Nuclear Magnetic Resonance (NMR), and UV-Vis and fluorescence spectrometry to assess this. The obtained measurements will guide the production of nanoparticles that contain active protein and a more homogenous assembly, which represents an innovative approach to nanoparticle production guided by protein structure analysis.

Background and Significance

Lipid nanoparticles (LNPs) are molecules that can deliver both hydrophobic and hydrophilic drugs inside cells, as well as introduce food additives or cosmetics.[1] Their size can go from 1 to 1,000 nm, making it easier for them to penetrate cell membranes and

carry different molecules into the cytosol.[2] They have many advantages over existing therapies, including improved loading capacity, controlled drug release, and high biocompatibility and biodegradability.[6,7] In addition, they have low cytotoxicity and can be easily modified to go undetected by the immune system.[2,8] Moreover, these nanoparticles can accumulate in different cells, making them potentially useful to treat intracellular infections such as Salmonella.[9] Some of the most studied LNPs due to their capacity as drug delivery systems are solid lipid nanoparticles (SLNs), nanostructured lipid carriers (NLCs), and liposomes.[10]

SLNs are colloidal carriers with a mean diameter between 50 and 1,000 nm.[11] They are prepared using lipids whose melting points are high so that they have a solid phase and have mechanical stability.[1,10] Figure 1 (left) shows the structure of an SLN. This kind of LNP has attracted increasing attention during recent years because of its high biocompatibility and biodegradability, as well as its low cost of production.[9] They also have high oral bioavailability and can be produced on a large scale by high-pressure homogenization.[11] Most recently, SLNs are being studied to be administered orally. However, to be efficient for oral administration, they first have to overcome the absorption barrier of the intestinal mucosa.[11] According to Yun et al., one way to do so is to modify them by adding Polyethylene glycol (PEG), a non-toxic and highly soluble molecule on water.[11]

NLCs, contrary to SLNs, combine at least one solid and one liquid phase, as well as a surfactant.[1] They can take several forms, including some with shells that can either be solid or liquid and others which structure intercalates solid and liquid phases.[6] Figure 1 (right) shows the structure of an NLC. These differences in structure affect the release

of drugs from the nanoparticle core, as NLCs with solid shells display low release and greater stability. On the other hand, particles with the liquid phase as “shell” will release the drug faster.[1] As LNPs, NLCs also have low toxicity and can contribute to the delivery of drugs inside the cells. For example, Sadegh et al. (2019) determined that these nanoparticles can help overcome the blood-brain barrier (BBB), a series of endothelial cells joined together by tight junctions.[12] This barrier, although useful for the protection of the central nervous system from harmful chemicals, limits the entry of drugs used to treat neurodegenerative diseases like Alzheimer's.[12] Therefore, using carriers such as NLCs can be effective in treating these illnesses.

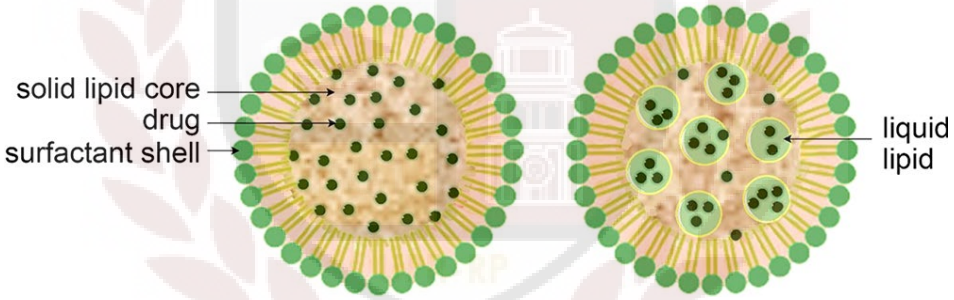

Figure 1: Structure of a solid lipid nanoparticle (left) and a nanostructured lipid carrier (right) [13]

Finally, liposomes are spherical vesicles formed by a lipid bilayer of phospholipids with an aqueous core, and their size ranges from 20 to 1,000 nm.[13,14] As SLNs and NLCs, liposomes are also able to transport hydrophobic and hydrophilic drugs. In their case, this is possible due to the amphipathic nature of phospholipids.[15] Another factor that affects this transport is the different modifications of the liposomes that give liposomes distinctive

functions.[16] Figure 2 shows the structure of some liposomal nanoparticles and the modifications they may have.

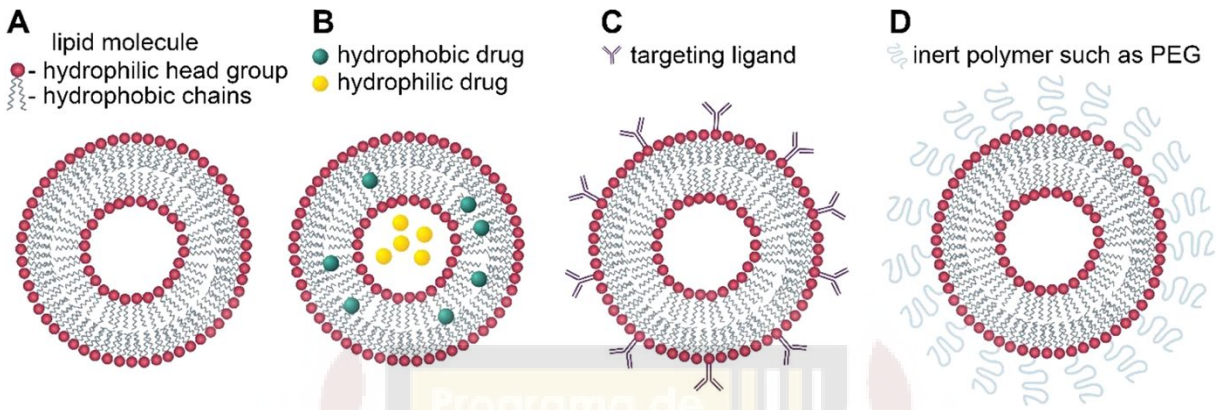

Figure 2: Structure of a liposome (A), a liposome encapsulating hydrophobic and hydrophilic drugs (B), immunoliposome functionalized with targeting ligands (C), and sterically stabilized liposome functionalized with inert polymers such as PEG (D) [14]

Another important characteristic of LNPs is that they can transport anticancer drugs with minimal side effects on healthy cells.[10] Vectorization of the nanocarriers can be achieved through passive or active targeting. The first one occurs when liposomes enter the tumoral cells by molecular movement through the cellular membrane. Active targeting, on the other hand, is achieved through structural modifications on the liposomes (often antibodies that recognize tumor cells). There is a third method, where the liposomes are prepared to respond to some condition changes that may be modified for the controlled delivery of the drugs using external triggers.[2]

A LNP of great interest for the present study is the complex created between cytochrome c (Cytc) and cardiolipin (CL). Cytc is an electron carrier in the mitochondrial respiratory chain capable of triggering apoptosis, while CL is a phospholipid found in the inner mitochondrial membrane that interacts with Cytc.[5,17] This interaction between Cytc and CL happens before apoptosis, and it seems to activate the peroxidase activity of

Cytc, therefore leading to apoptosis.[5] Also known as programmed cell death, apoptosis is a mechanism that cells have evolved to commit suicide in dangerous conditions.[19] Through this mechanism, living organisms can remove damaged cells, including cells transformed to cancer cells.[19] There are a few ways in which apoptosis could proceed, but according to Vladimirov et al. (2011), it always entails the permeabilization of the mitochondrial membrane and the release of cytochrome c into the cytosol.[18]

Studies have shown that the binding of CL to Cytc is what causes this protein to act as a peroxidase. However, how these two molecules bind and the changes that their binding produces on the structure of Cytc is undetermined.[20] Something important about these processes is that most peroxidases exist in a pentacoordinate form that allows H_2O_2 to bind by the sixth coordination bond.[21] These hemoproteins show greater peroxidase activity than that of Cytc, as the sixth coordination bond in Cytc (Fe^{2+}) is occupied by its Met80.[21] Another important detail is that cardiolipin enhances peroxidase activity, promotes the oxidation of Cytc, and accelerates oxidation of Cytc (Fe^{2+}) to Cytc (Fe^{3+}) by breaking the Fe and S (Met80) bond, and the system of conjugated bonds in the heme porphyrin ring.[21] This enhancement of the peroxidase activity, in turn, leads to more significant apoptotic activity and may challenge anti-apoptotic events.

Researchers have proposed a two-step process for the release of Cytc. The first step is the disruption of the interaction of Cytc and CL to solubilize the protein. Studies propose that the interaction of these two molecules happens in two particular regions of Cytc: the A-site (Lys72, Lys73, Lys86, Lys87, and Arg91) and the L-site (Lys22, Lys, 25, Lys27, His26, and His33). These interactions are due to electrostatic attractions.[22] Two possible models have been proposed in terms of the structure. The first one proposes

that Cytc is bound to the surface of a cardiolipin-containing membrane due to electrostatic attraction.[22] Figure 3a shows how this possible assembly may look. Opposed to this model, a second one suggests that Cytc not only binds to the surface of the lipid layer, but it winds the layer around itself to form the spherical nanosphere.[22] Figure 3b shows this second model of binding.

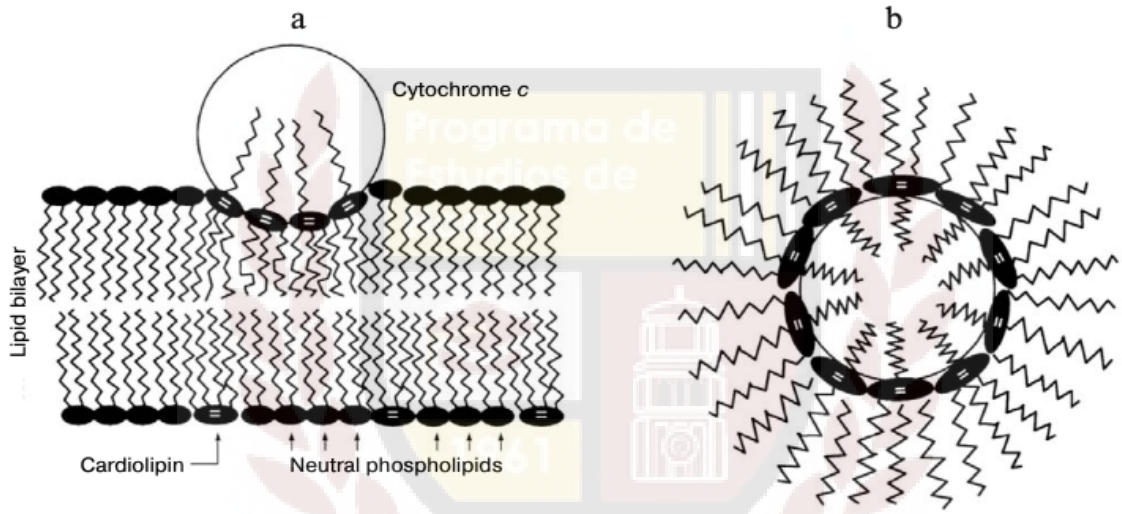

Figure 3: (a) Cytochrome c attaches to the membrane containing cardiolipin by electrostatic attraction. (b) Cytochrome c binds the membrane lipid layer around itself

The second step for the release of Cytc into the cytosol is the permeabilization of the outer mitochondrial membrane and happens right after the interactions between Cytc and CL are disrupted. The permeabilization of this membrane is possible thanks to pro-apoptotic proteins belonging to the family of Bcl-2 proteins, which are involved in the regulation of the release of mitochondrial factors that result in apoptosis and may be pro-apoptotic or anti-apoptotic.[24] Specifically, the proteins Bax (Bcl-2-associated X protein) and Bak (Blc-2-antagonistic killer) are the ones that permeabilize the membrane. Bax

resides in the outer membrane of the mitochondria, while Bak is found in the cytosol.[25] Studies propose that Bax forms large clusters of approximately 250 to 600 nm diameter and inserts itself into the outer membrane to permeabilize the membrane. Unfortunately, the specific mechanism of this process is still unknown.[25] This process is of great significance, as the release of Cytc into the extramitochondrial environment will lead to the interaction between the protein and Apaf-1 and activate pro-caspase-9. This last molecule will activate pro-caspase 3, which leads to other processes and transformations that result in the death of the cell.[26] The entire two-step process of the release of Cytc from the mitochondria is shown in figure 4.

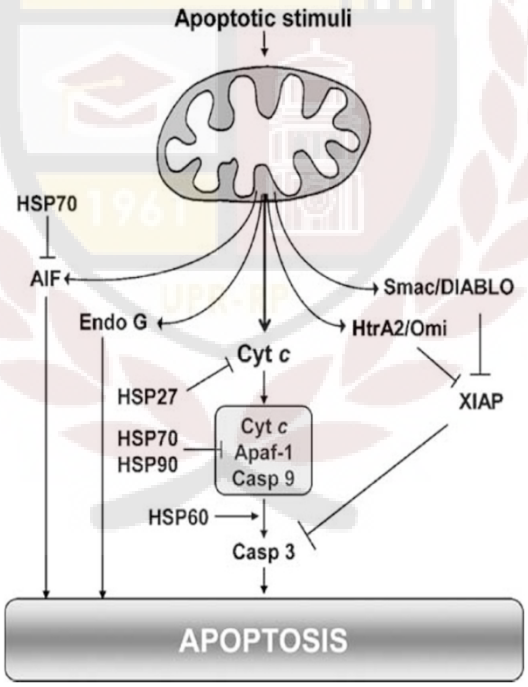

Figure 4: Two-step process of the release of Cytc from mitochondria.[27]

In cancer cells, the process of apoptosis does not occur as in healthy cells. Mainly, this happens because cancer cells overexpress anti-apoptotic proteins, such as the B-cell/lymphoma 2 (Bcl-2) family that will prevent the permeabilization of the outer

mitochondrial membrane and the release of Cytc as a consequence of this.[28] Based on that, new anticancer methods suggest going against these anti-apoptotic proteins by using Cytc delivery systems such as polymer-based nanoparticles or LNPs to transport this protein inside the cell. The nanoparticle composed of Cytc and CL, the Cytc-CL complex, is known to initiate apoptosis following different pathways. One of these possible courses is the particle's penetration on the cell membrane and into the cytoplasm and the liberation of Cytc to initiate cell death. On the other hand, the process could also begin with lipid peroxidation within the cytoplasmic and mitochondrial membranes.[28]

In 2020, female breast cancer was denominated the leading cause of global cancer incidence[3]. It is the principal cause of cancer death among Hispanic women, with them being less likely to be diagnosed at a local stage.[29] Some of the most common treatments for cancer are surgery, radiotherapy, chemotherapy, hormone therapy, immunotherapy, and targeted therapy.[29] However, the effects of these procedures may not only disturb the tumor tissue, but also normal tissue, leading to systemic toxicity and adverse effects.[4] Therefore, innovative alternatives to fight off cancer have been under study during past years. One of these possible therapies is the use of lipid nanoparticle delivery systems, which could induce apoptosis and kill cancer cells.[30]

Theoretical Frame

Nanoparticle homogeneity

The stability of nanoparticles is defined in terms of aggregation, shape, size, surface chemistry, among other factors.[41] In the process of producing LNPs to use them

as drug carriers, an important characteristic that may be evaluated is the homogeneity of the complex is studied through Dynamic Light Scattering (DLS). DLS allows the study of nanoparticle homogeneity measuring the polydispersity index (PDI) of the sample. The PDI is a numerical representation of the distribution of size populations.[42] The value may vary from 0.0 (for a perfectly uniform sample in terms of particle size) to 1.0 (for a polydisperse sample with multiple particle sizes). Generally acceptable values of PDI for LNPs are 0.3 and below.[42] A central hypothesis of this project is that the homogeneity of Cytc-encapsulating lipid nanoparticles can be modulated by the specific lipid composition. Furthermore, recapitulating the lipid composition that accompanies native Cytc-CL interactions in mitochondria may result in optimal nanoparticle assembly.

Characteristics of biological membranes

Cell membranes are a primary component of the cell, as they act as the most external envelope for the cell, protect the intracellular space from the extracellular environment, and help compartmentalize organelles.[31,32] One of the most influential models of cell membranes is the fluid mosaic membrane model, which was presented in 1972. According to this model, the membrane has many proteins within a uniform leaflet of lipids, however, it is known that a variety of lipids can be found in the leaflets.[33] It has been determined that the lipid composition of the membranes can vary, which implies that they will have different physical functionalities and lead to a variety of biological functions.[34] In addition, these lipids and their amphipathic nature are what cause the cell membrane to be arranged as a lipid bilayer.[35] The lipid bilayer can incorporate proteins in both the hydrophilic and hydrophobic parts of the membrane, as well as proteins that span from one side to the other.[34]

Cell membranes also help control the transport of molecules across cell and organelle surfaces, something that is essential for cell function and many biological

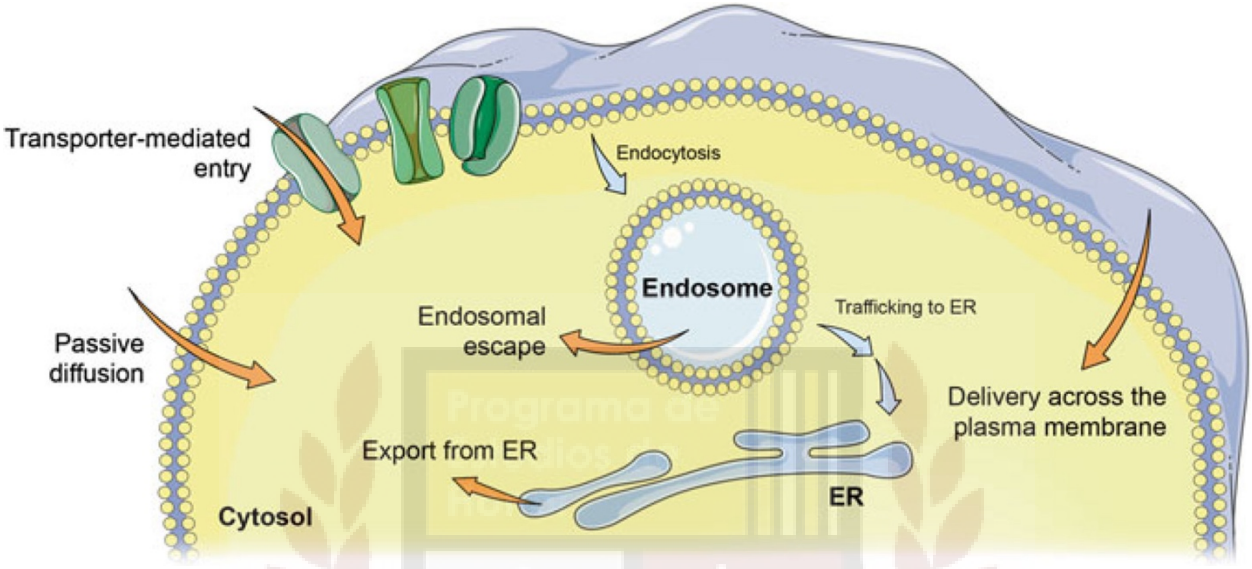

Figure 5: Possible routes of entry into the cytosol.[36]

processes. Figure 5 shows some of the possible routes for transport inside the cells. The most commonly studied are active and passive transport, where active transport requires an energy input to translocate molecules against their concentration gradients, while passive transport does not require any additional energy.[36] Passive transport can happen through simple lipoidal transport, channel-mediated diffusion, and carrier-mediated diffusion.[32] This type of transport is understood in the context of Overton's rule, which states that membrane permeability is proportional to the product of diffusivity and oil/water partition coefficient ($K_{o/w}$) of a permanent molecule, and it is the most common route for drugs to enter cells. However, some molecules cannot diffuse passively across the cell membrane due to their size and polarity. Lipid and polymer-based nanoparticles may result helpful in these cases, as they can increase the permeability of these molecules through the bilayer membrane.[2,36]

Mitochondrial membranes: Lipid composition

The lipidomic composition of the cell membrane may vary depending on the tissue or even on intracellular membranes.[31] An evident example of this is the mitochondria, which have two membranes: the outer mitochondrial membrane (OMM) and the inner mitochondrial membrane (IMM). The IMM is the active site for the electron transport chain and where ATP production happens.[37] It also has a high number of membrane-associated proteins, with an estimated protein-lipid ratio of 3:1.[37] In the mitochondria, we can find a variety of lipids, although the most abundant ones are PC, PE, and CL. Figure 6 shows the lipids found in the inner and outer membrane of the mitochondria.

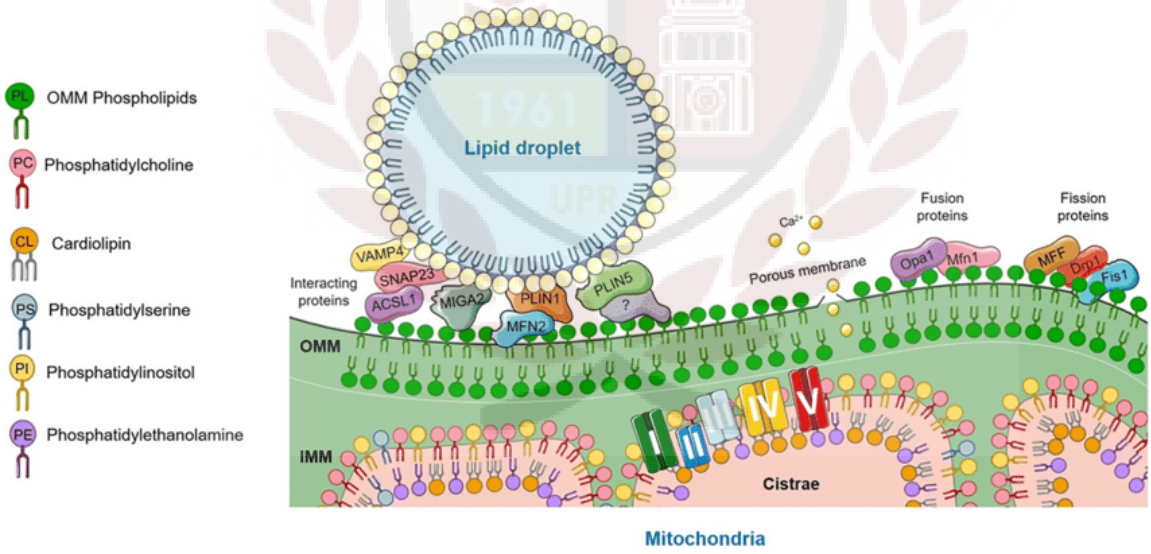

Figure 6: Lipids found in the outer mitochondrial membrane (OMM) and the inner mitochondrial membrane (IMM).[38]

CL is of great importance among these lipids because of its role in programmed cell death, also known as apoptosis.[5] CL is an anionic phospholipid with a

diphosphoglycerol headgroup and four acyl chains (Figure 7). A distinctive feature about CL is the sharing of the glycerol molecule by two phosphatidate moieties, which reduces the size of the polar group and promotes greater cohesion between the CL hydrocarbon chains, and results in a higher melting temperature.[39] Some of the main functions of this lipid are the segregation of membrane domains and the formation of nonlamellar structures.[40]

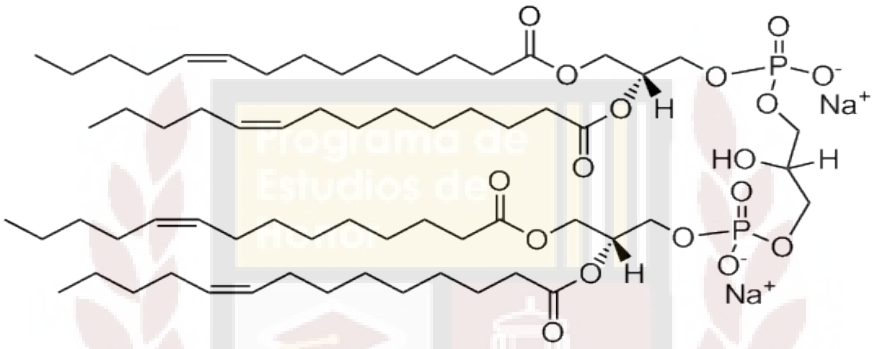

Figure 7: Structure of cardiolipin

Justification

The most common treatments for breast cancer are surgery, radiotherapy, chemotherapy, and targeted therapies for some subtypes. These treatments often affect tumor tissue, as well as healthy tissue, which may lead to systemic toxicity and have adverse effects.[4] As this illness becomes one of the most common cancers diagnosed among women, novel therapies are needed to eradicate cancer cells.[14,29] A promising treatment is the use of LNPs to induce apoptosis in cancer cells, something they cannot do on their own. Of particular interest for this study is the Cytc-CL complex, which has proven to induce apoptosis through peroxidase activity.[5] For proper use of these nanoparticles as drug delivery systems for cancer treatment, vast knowledge of the

nanoparticle structure and the process behind its pro-apoptotic behavior is necessary. However, recent studies performed to understand the cytotoxic character of Cytc-CL nanoparticles fail to use rigorous characterization methods and provide structural information about them.

To address this issue, we expect to develop a therapeutic protein delivery system that takes advantage of the proapoptotic activity of Cytc and CL to treat breast cancer. Through our innovative approach, we aim to preserve the native interactions between Cytc and CL in nanoparticle formulations, and to optimize this production of the Cytc-CL complex through an extensive structural analysis using different characterization methods and procedures to study nanoparticle morphology. This innovative method for the preparation of LNPs as drug delivery systems will provide important structural information about the nanoparticle we are studying. Not only will it allow a better understanding of the nanoparticle's structure, but it will also help predict the behavior of the molecule within determined chemical environments. That is of great importance for the use of nanoparticles as cancer treatments, as it will allow us to assess its apoptotic action in cancer cells.

Methodology

Aim: To optimize the production of Cytc-CL nanoparticles based on structural analysis

Experimental Design: To fulfill our Aim, we used the following experimental design:

1. Preparation of lipid-protein conjugates

To prepare nanoparticles by complexing Cytc with different molar excesses of CL (TOCL, CAS 115404-77-8), PC (PC, CAS 26853-31-6), and PE (POPE, CAS 26662-94-2), a phosphate buffer solution was first diluted from a concentration of 1M to 10mM. After this dilution, using three separate tubes, 1.0mg of Cytc from bovine heart (Cytc, CAS 9007-43-6) were added and dissolved in 1.9mL of the buffer. Different molar excesses of the lipids over Cytc were calculated, and the required mass was weighed and dissolved in methanol, keeping the alcohol concentration at a value lower than 5%v/v (0.1mL will be used in every tube). Each of these formulations were added drop-by-drop to each of the three tubes containing Cytc while stirring. This mixture was subjected to sonication for 4 minutes. A control solution of each lipid particle was prepared following the same procedure, as well as a control solution for the protein alone.

Sample preparation methods also included centrifugation and extrusion. Centrifugation was performed at 12,000 rpm and a temperature of 25 ºC for 5 minutes. Extrusion, on the other hand, was accomplished using an Avanti® Mini-Extruder. For that method, the nanoparticle solution was passed repeatedly through a polycarbonate membrane with a pore diameter of 0.2 µm. This created liposomes with a diameter close to the size of the pores.

2. *Characterization of CL: Cytc nanoparticles*

2.1. *Dynamic Light Scattering (DLS)*. Particle size and polydispersity index (PDI) were measured using a Nano ZS90 Zetasizer (Malvern Instruments) equipment at 25ºC to determine if we had a homogenous population of nanoparticles. DLS samples

of the nanoparticles were evaluated after sonication, and then after centrifugation and extrusion were performed. Control solution's measurements were also taken. Size distribution by intensity for each sample was obtained, with graphs showing the results obtained from three measurements of each sample.

2.2. *Scanning Electron Microscopy (SEM)*. Samples for SEM analysis were prepared and processed as reported by Piroeva et al[43]. Following is a brief description of each step.

Sample fixation and dehydration. A coverslip (18 x 18 mm^2) was used as a platform for nanoparticle fixation. The coverslip was dipped in a 0.8 % agar solution and left horizontally, allowing the thin agar film to materialize for 30 minutes. Nanoparticles samples were deposited on the agar film and allowed to settle for 45 minutes. The samples were then dehydrated in an oven at 37 °C for 12 hours.

Gold coating. Fixed and dehydrated samples were coated with a thin gold film (~10 nm) using a metal sputter system.

SEM analysis. SEM imaging was performed with the high-resolution field emission scanning electron microscope (JEOL JSM-7500F SEM), using 2 kV (unless otherwise specified) acceleration voltage for a gentle electron beam. The sample (coverslip) was mounted on a double-coated conductive carbon tape that holds the sample firmly to the stage surface and a copper tape was placed as a ground strap from the sample surface to the SEM sample holder.

2.3. *Liquid-state Nuclear Magnetic Resonance (NMR).* Solution NMR spectra were recorded at 500MHz ^{1}H Larmor frequency in a Bruker Aeon spectrometer equipped with a HX Double Resonance Prodigy Cryoprobe. The measurements assessed lipid-protein interactions, as evidenced by shifts in the spectra with respect to lipid-only formulations.

2.4. *Fluorescence and UV-Vis Spectrophotometry.* To determine the oxidation state of the nanoparticle, we measured fluorescence and UV-Vis spectra. Fluorescence was be measured using a spectrofluorophotometer (Shimadzu RF-5301PC) and UV-Vis was measured using a NanoDrop™ 2000 Spectrophotometer (Thermo Scientific™).

Results and Discussion

Dynamic Light Scattering (DLS)

Particle size and Polydispersity Index (PDI)

Following the preparation of the CL: Cytc nanoparticles, the particle size and PDI of each sample were measured using a Malvern Nano ZS90 Zetasizer. Particle size for the nanoparticles ranged from 65.9 nm to 209.9 nm, with an average size of 92.36 nm for CL: Cytc nanoparticles, 116.52 nm for PC: Cytc nanoparticles, and 181 nm for PE: Cytc nanoparticles. The standard deviation values for these measurements were 64.23 nm, 57.03 nm, and 69.13 nm, respectively. Nevertheless, polydispersity index is the metric

typically used in DLS analysis. PDI is defined as the square of the standard deviation divided by the square of the mean. In terms of PDI, the values ranged from 0.073 to 0.443, with an average PDI value of 0.294 for CL: Cytc nanoparticles, 0.203 for PC: Cytc nanoparticles, and 0.138 for PE: Cytc nanoparticles (Table 2). Therefore, CL: Cytc nanoparticles were the smallest in particle size, but the most polydisperse in comparison to formulations with PC or PE. Graphs of size distribution by intensity for each nanoparticles sample and control solution are presented in Appendix A.

Control	DLS preparation process	Mean particle size (d. nm)	Polydispersity Index value (PDI)
Cytc	Sonication	5.864	0.361
	Centrifugation	N/A	N/A
	Extrusion	293.9	0.449
CL	Sonication	793.6	0.696
	Centrifugation	481.9	0.539
	Extrusion	145.4	0.142
PC	Sonication	N/A	N/A
	Centrifugation	691.8	0.372
	Extrusion	246.8	0.374
PE	Sonication	5378	0.346
	Centrifugation	872.2	0.676
	Extrusion	145.2	0.395

Table 1: Summary of particle size and polydispersity index values of the control solutions

Lipid: Cytc (mole: mole)	DLS preparation process	Mean particle size (d. nm)	Polydispersity Index value (PDI)
CL: Cytc 25:1	Sonication	74.91	0.443
	Centrifugation	65.94	0.432
	Extrusion	72.97	0.318
CL: Cytc 35:1	Sonication	100.1	0.231
	Centrifugation	95.34	0.220
	Extrusion	95.34	0.221
CL: Cytc 45:1	Sonication	105.3	0.215
	Centrifugation	127.8	0.362
	Extrusion	93.52	0.205
PC: Cytc 25:1	Sonication	119.0	0.251
	Centrifugation	106.6	0.137
	Extrusion	104.7	0.152
PC: Cytc 35:1	Sonication	108.4	0.229
	Centrifugation	101.1	0.152
	Extrusion	98.16	0.145

PC: Cytc 45:1	Sonication	145.8	0.328
	Centrifugation	139.1	0.248
	Extrusion	125.8	0.185
PE: Cytc 25:1	Sonication	N/A	N/A
	Centrifugation	152.8	0.127
	Extrusion	152.8	0.127
PE: Cytc 35:1	Sonication	N/A	N/A
	Centrifugation	209.9	0.107
	Extrusion	181.0	0.073
PE: Cytc 45:1	Sonication	3.614	0.271
	Centrifugation	183.8	0.120
	Extrusion	205.7	0.204
PC: CL: Cytc 85:15, 45:1 Lipid: Cytc	Centrifugation	56.64	0.355
	Extrusion	65.31	0.442
PC: PE: CL 55:30:15, 45:1 Lipid: Cytc	Centrifugation	122.1	0.272
	Extrusion	133.2	0.293

Table 2: Summary of particle size and polydispersity index values of the nanoparticles formulations

Lipid composition (molar fractions)

To study the effect of different lipid: protein molar fractions in size and polydispersity, we prepared formulations of 25:1, 35:1 and 45:1 lipid to Cytc ratios. Size distribution by intensity of the different molar fractions of each lipid type were compared and we observed that for all the lipids, the molar ratio of 25: 1 had the smallest nanoparticle sizes (Figures 8, 9 and 10). A trend in terms of PDI with respect to lipid: protein molar fractions was not observed (Table 2).

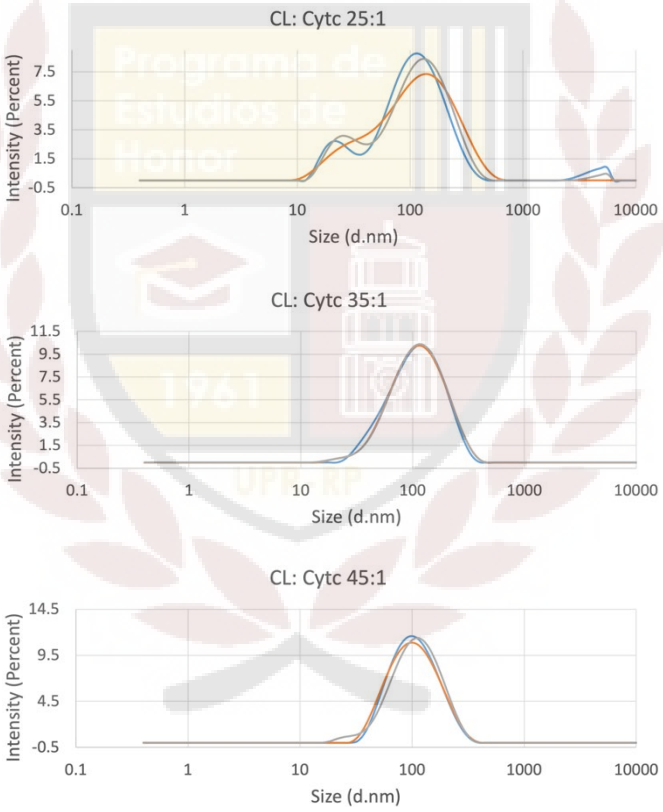

Figure 8: CL: Cytc nanoparticles with different molar fractions of lipid: protein.

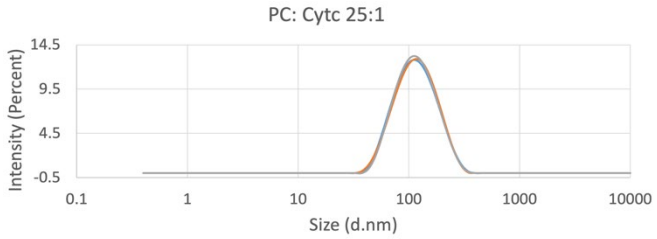

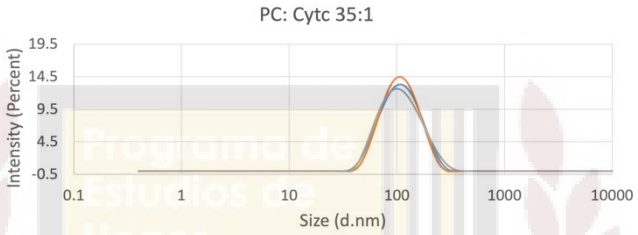

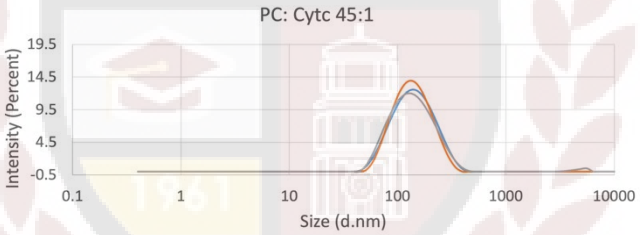

Figure 9: PC: Cytc nanoparticles with different molar fractions of lipid: protein.

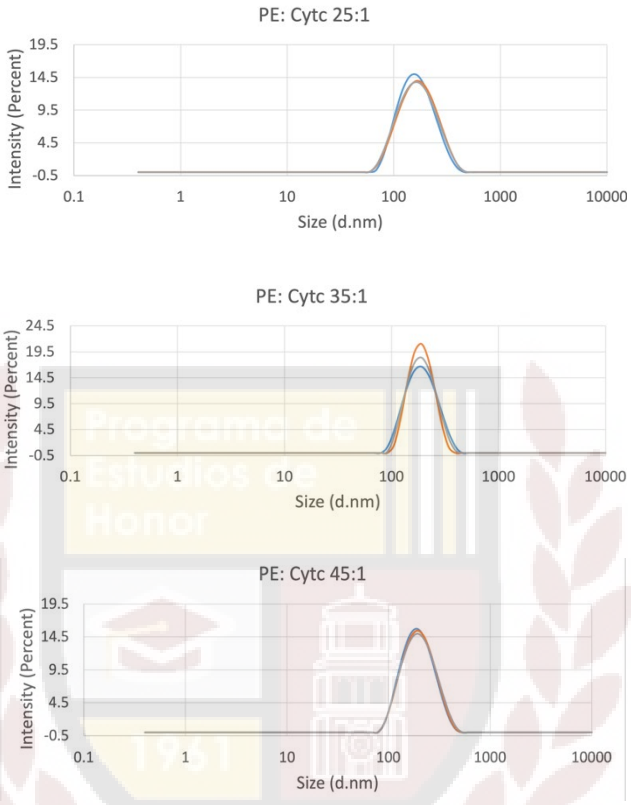

Figure 10: PE: Cytc nanoparticles with different molar fractions of lipid: protein

Lipid composition (lipid identity)

Interactions between CL and Cytc, as well as the other lipids when complexed in a nanoparticle, were studied to see how these may affect the particle size and homogeneity of our samples. When comparing the size distribution by intensity of nanoparticles formulations with different lipids, we observed that nanoparticles with CL had a smaller size, followed by PC and PE, respectively (Figure 11). PDI values, on the other hand, were the highest for nanoparticles with CL, followed by PC and PE (Table 2).

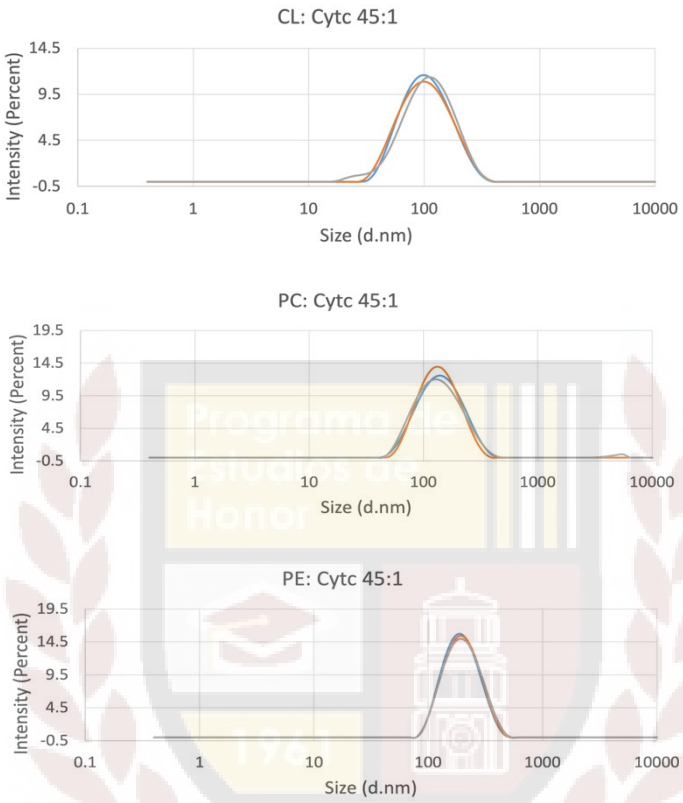

Figure 11: 45:1 Lipid: Cytc nanoparticles with different lipids.

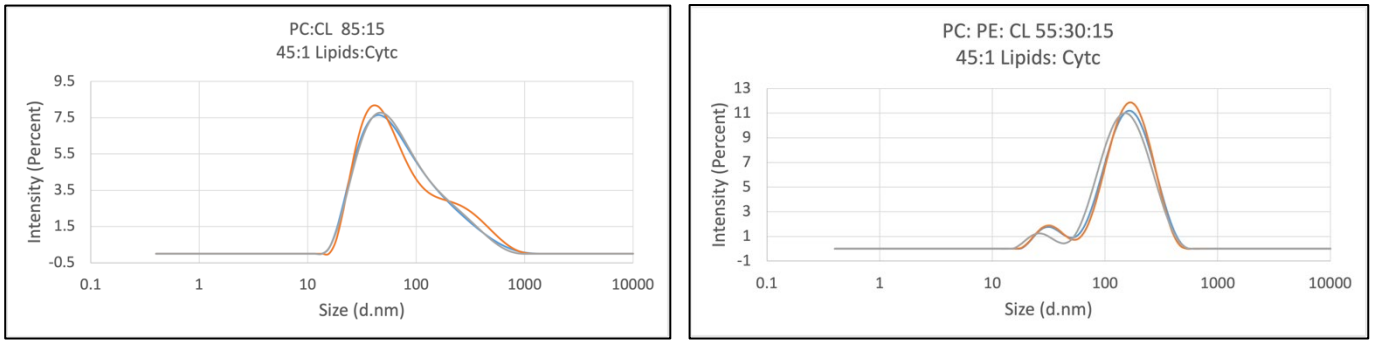

Figure 12: 45:1 Lipid: Cytc nanoparticles with different lipid compositions (PC:CL 85:15 on the left and PC: PE: CL 55:30:15 on the right)

Sample preparation methods

When preparing our samples, we used three different methods to see which provided a smaller particle size and a more homogenous sample: sonication, centrifugation, or extrusion. As observed in the figures below (Figures 13, 14 and 15), sample homogeneity improves when extrusion is performed. Nanoparticle size is also decreased in most cases when samples are extruded.

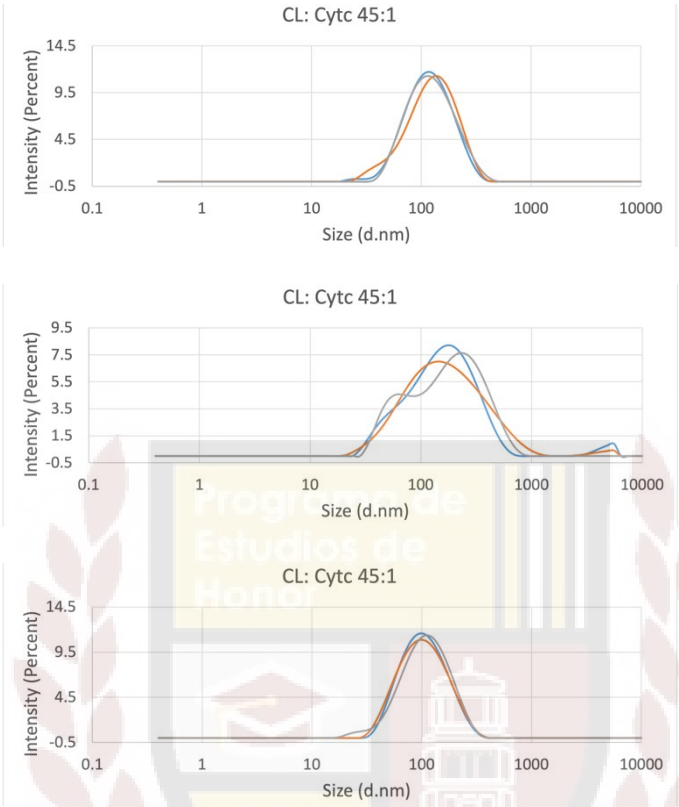

Figure 13: CL: Cytc 45:1 nanoparticles solution prepared by sonication, centrifugation, and extrusion.

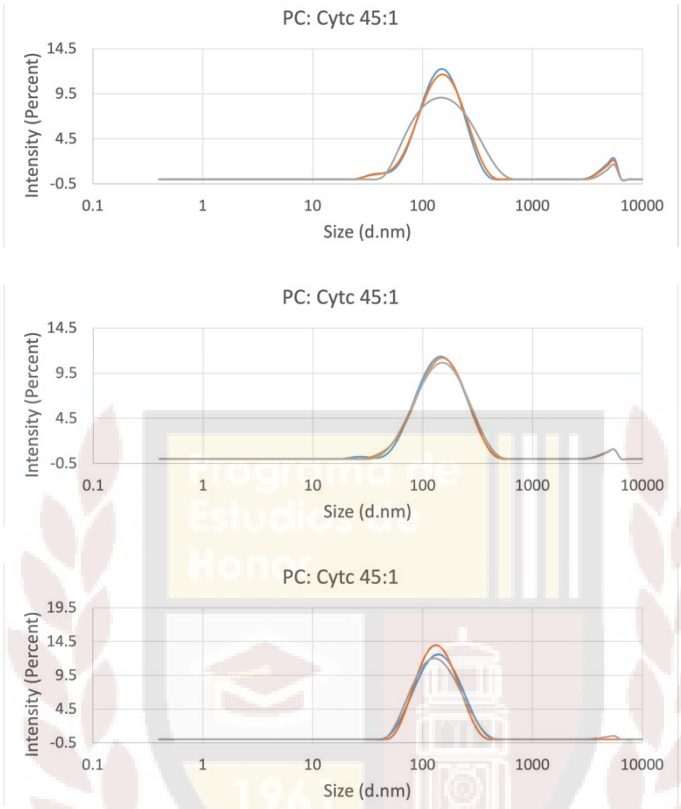

Figure 14: PC: Cytc 45:1 nanoparticles solution prepared by sonication, centrifugation, and extrusion.

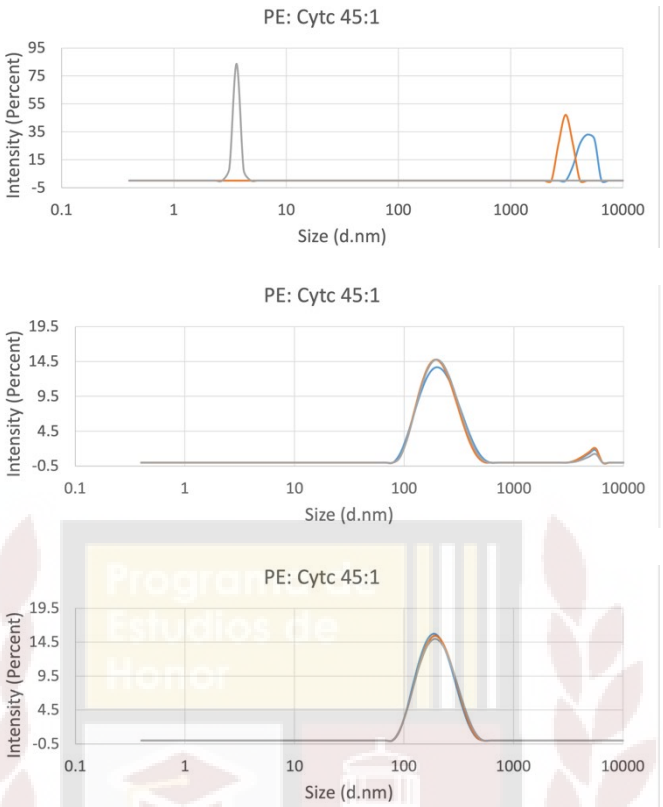

Figure 15: PE: Cytc 25:1 nanoparticles solution prepared by sonication, centrifugation, and extrusion.

Scanning Electron Microscopy (SEM)

SEM analysis was performed for each nanoparticles samples. Low-resolution images were obtained; however, an approximately spherical shape was observed for CL: Cytc nanoparticles. According to the SEM micrograph in Figure 16, the diameter of this nanoparticle is of around 350 nm.

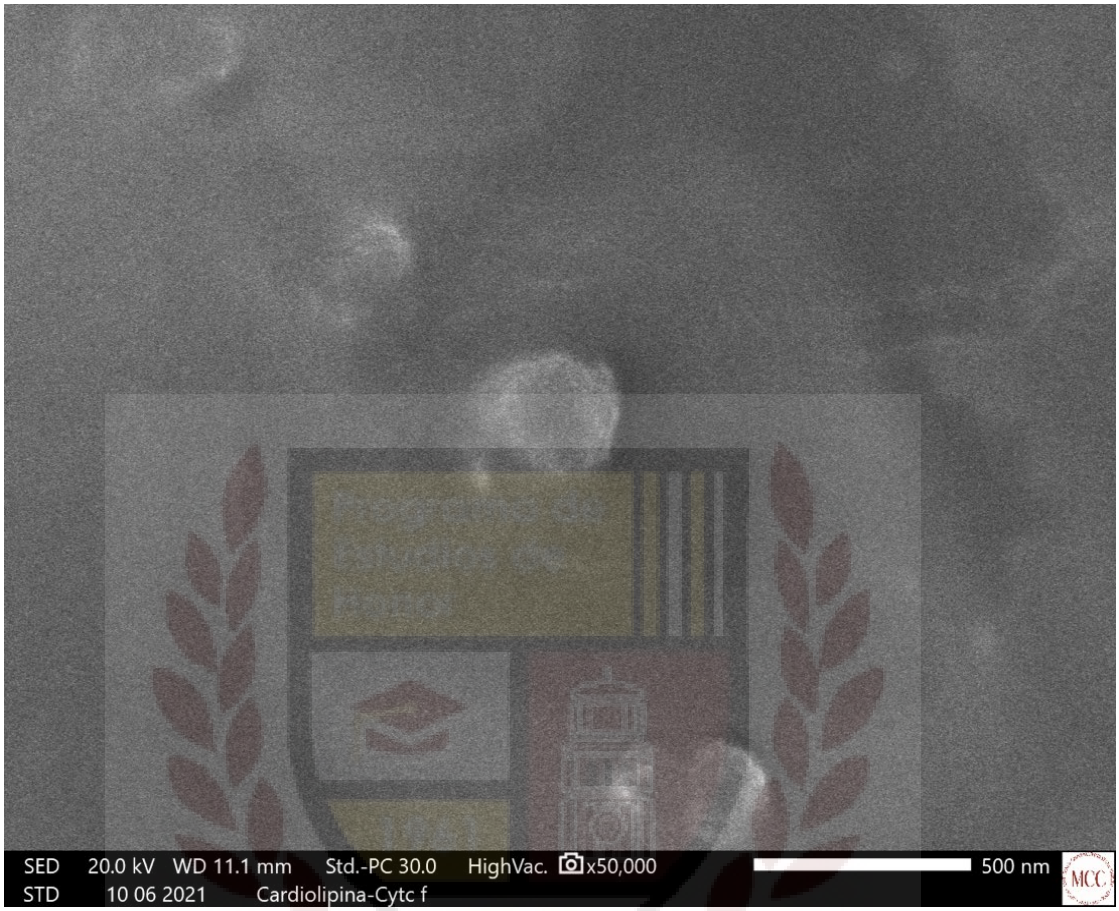

Figure 16: Scanning electron micrograph of CL: Cytc 45:1 complex. Scale bar: 500 nm.

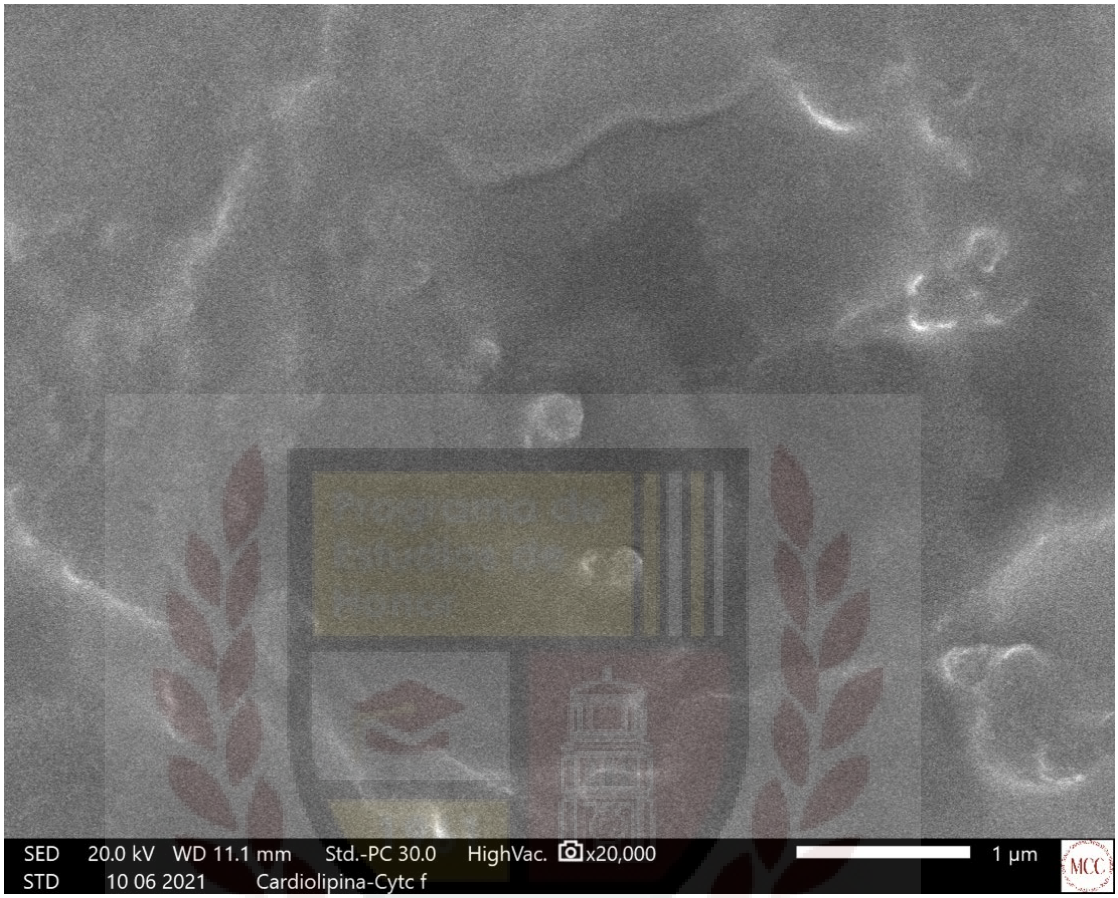

Figure 17: Scanning electron micrograph of CL: Cytc 45:1 complex. Scale bar: 1 μm.

Liquid-state Nuclear Magnetic Resonance (NMR)

^{1}H NMR spectra was recorded for control and nanoparticles solutions at 500MHz ^{1}H Larmor frequency and 25°C. First, we observed that, keeping equal concentrations of Cytc, the sample with CL: Cytc nanoparticles lacks signals from the protein in solution NMR spectra, as illustrated in Figure 18. The disappearance of protein signals is consistent with the incorporation of protein molecules onto the nanoparticle complex, which exhibits a much higher rotational correlation time that eliminates NMR signals in solution. However, lipid molecules that form nanoparticles are free to rotate and diffuse

on the surface, lowering their correlation time and permitting their observation in solution NMR spectra. In Figure 19, the aliphatic region of ^{1}H NMR spectra showing signals from CL is shown. Signal assignments derived from Alexandri et al.[44] A signal displacement for CL: Cytc assemblies for various molar fractions relative to pure CL is observed. This may be due to lipid-protein interactions and the presence of an excess of lipids in relation to Cytc.

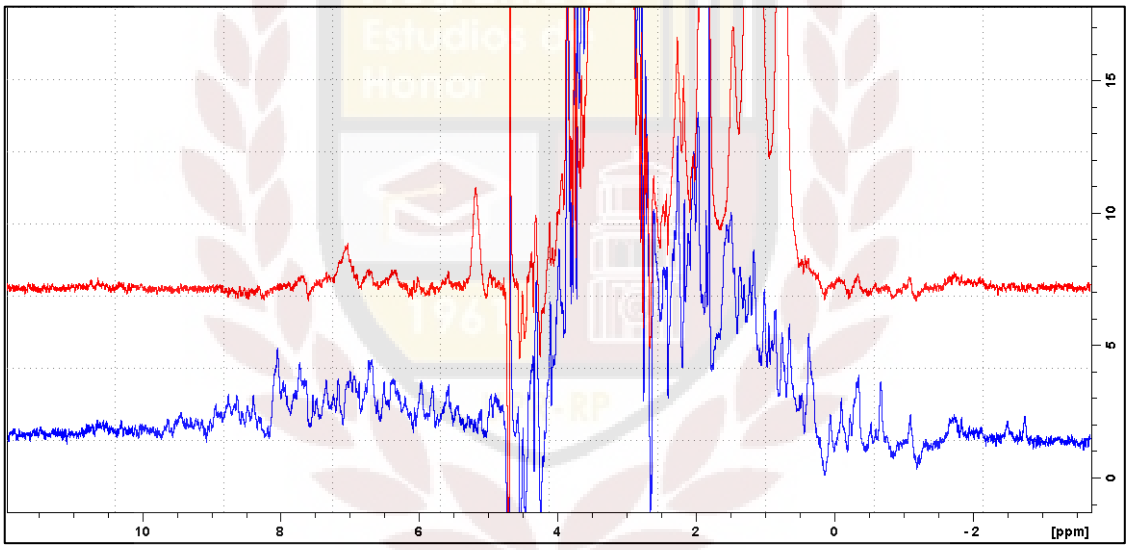

Figure 18: Solution ^{1}H NMR spectra of CL: Cytc (top) and Cytc only (bottom) solutions

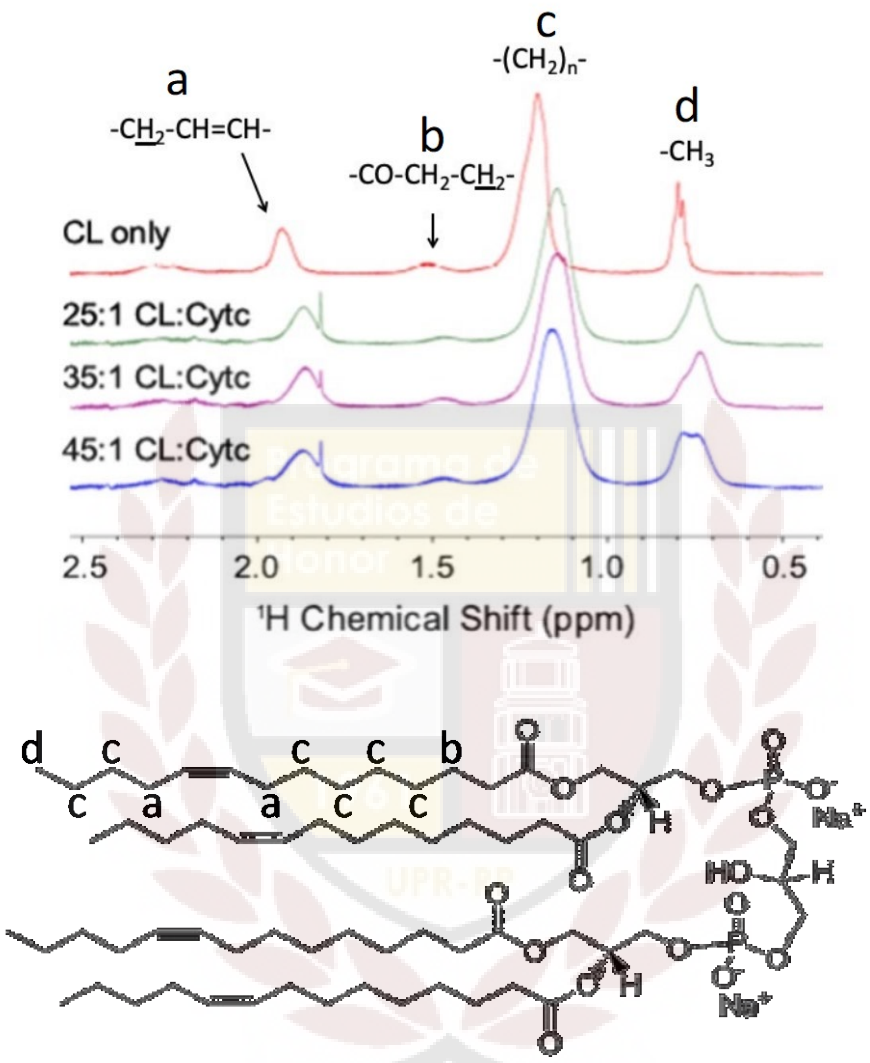

Figure 19: Solution ^{1}H NMR spectra of CL: Cytc complexes (left) and cardiolipin molecular structure with labelled 1H species (right) [7]

Conclusion

Lipid nanoparticles of CL: Cytc, among other formulations, were prepared in-vitro to test the hypothesis that the electrostatic interactions that guide native protein-lipid association will lead to the homogeneous assembly of protein-lipid liposomes. After analyzing these samples by DLS, SEM, and NMR, we conclude that homogenous samples were achieved. First, through DLS analysis, we established that particle size ranged from 65.9 nm to 209.9 nm, with the smallest being CL: Cytc nanoparticles. In terms of PDI, the most effective sample preparation method was extrusion, with PDI values of 0.318 or less for nanoparticles with CL, PC or PE (Table 2). SEM imaging facilitated the recognition of nanoparticles shape, which was approximately spherical (Figures 15 and 16). Finally, solution NMR spectra were recorded for the nanoparticles and compared to those of lipid-only solutions. In these spectra, the most prominent signals were from aliphatic sites, due to their inherent flexibility. Aliphatic 1H signals shifted in the complexes relative to the CL and are attributed to lipid-protein interactions (Figure 17). In summary, the results obtained through this study help elucidate which formulations and methods result in more homogenous assembly of nanoparticles that can later be employed as treatment for breast cancer cells. These are nanoparticles with molar ratios of lipid: protein of 45:1 and prepared using extrusion method.

Future works include acquiring UV-Vis spectroscopy and fluorescence spectrophotometry data, which we did not achieve due to equipment malfunctions. We also plan on studying cytotoxicity levels and cell viability of breast cancer cells after being treated with CL: Cytc. Further studies involve the identification of the targeting method

our nanoparticle will use to ensure that it only attacks cancer cells, without affecting adjacent healthy tissue. Something we are contemplating is the use of antibodies as ligands on the liposome to target cells transformed to cancer cells. These studies should contribute important information about the apoptotic ability of CL: Cytc nanoparticles and their potential as a cancer treatment.

Acknowledgements

I'm incredibly thankful to Dr. Marvin J. Bayro, whose mentorship and encouragement have led to this achievement. His words of wisdom and ongoing support were of great help during the process of preparing my proposal and eventual thesis project. I also want to extend my sincere gratitude to Dr. Esther Peterson and Dr. Juan Ramírez, whose feedback and advice allowed me to improve my work during the past year. Special thanks to Dr. Jose Rodríguez and Dr. Elaine Alfonso for their constant guidance as part of the Honors Program and the opportunity I received as a member of this group of students.

I gratefully acknowledge the technical contributions of the Material Characterization Center (MCC), NIEF Image, and Dr. Eduardo Nicolau's laboratory. If it were not for their support and materials, this project could not have been possible.

Special gratitude to my graduate student mentor, Jemily Acosta, with whom I have worked for the past year and whose knowledge and guidance allowed me to fulfill this goal. I would also like to thank the entire Protein NMR Group, my friends and partners in the laboratory, whose unparalleled support often motivated me to keep working. Lastly, but of utmost importance, I want to thank God for His unwavering support and guidance, my family for being loving and patient during difficult moments, and my friends for always believing in me and never allowing me to give up.

This work was supported in part by funds from the Puerto Rico Science, Technology and Research Trust award 2020-00128 and the UPR Institutional Funds for Research (FIPI) Program to the Bayro research group. Graduate student mentor Jemily Acosta was supported by the RISE Fellowship under NIGMS-RISE 5R25GM061151-19 grant from the National Institutes of Health (NIH) to UPR Rio Piedras.

Works cited

(1) Dan, N. Nanostructured Lipid Carriers: Effect of Solid Phase Fraction and Distribution on the Release of Encapsulated Materials. *Langmuir* **2014**, *30* (46), 13809–13814. https://doi.org/10.1021/la5030197.

(2) García-Pinel, B.; Porras-Alcalá, C.; Ortega-Rodríguez, A.; Sarabia, F.; Prados, J.; Melguizo, C.; López-Romero, J. M. Lipid-Based Nanoparticles: Application and Recent Advances in Cancer Treatment. *Nanomaterials (Basel, Switzerland)* **2019**, *9* (4), 638. https://doi.org/10.3390/nano9040638.

(3) Sung, H.; Ferlay, J.; Siegel, R.L; Laversanne, M.; Soerjomataram, I.; Jemal, A.; Bray, F. Global Cancer Statistics 2020: GLOBOCAN Estimates of Incidence and Mortality Worldwide for 36 Cancers in 185 Countries. *CA: a cancer journal for clinicians* **2021,** *71* (3), 209-249. https://doi.org/10.3322/caac.21660

(4) Ewertz, M.; Jensen, A. B. Late Effects of Breast Cancer Treatment and Potentials for Rehabilitation. *Acta oncologica (Stockholm, Sweden)* **2011**, *50* (2), 187–193. https://doi.org/10.3109/0284186X.2010.533190.

(5) Marchenkova, M. A.; Dyakova, Y. A.; Tereschenko, E. Yu.; Kovalchuk, M. v; Vladimirov, Y. A. Cytochrome c Complexes with Cardiolipin Monolayer Formed under Different Surface Pressure. *Langmuir* **2015**, *31* (45), 12426–12436. https://doi.org/10.1021/acs.langmuir.5b03155.

(6) Guilherme, V. A.; Ribeiro, L. N. M.; Alcântara, A. C. S.; Castro, S. R.; Rodrigues da Silva, G. H.; da Silva, C. G.; Breitkreitz, M. C.; Clemente-Napimoga, J.;

Macedo, C. G.; Abdalla, H. B.; Bonfante, R.; Cereda, C. M. S.; de Paula, E. Improved Efficacy of Naproxen-Loaded NLC for Temporomandibular Joint Administration. *Scientific Reports* **2019**, *9* (1), 11160. https://doi.org/10.1038/s41598-019-47486-w.

(7) Kundu, P.; Das, M.; Tripathy, K.; Sahoo, S. K. Delivery of Dual Drug Loaded Lipid Based Nanoparticles across the Blood–Brain Barrier Impart Enhanced Neuroprotection in a Rotenone Induced Mouse Model of Parkinson's Disease. *ACS Chemical Neuroscience* **2016**, *7* (12), 1658–1670. https://doi.org/10.1021/acschemneuro.6b00207.

(8) Han, Y.; Li, Y.; Zhang, P.; Sun, J.; Li, X.; Sun, X.; Kong, F. Nanostructured Lipid Carriers as Novel Drug Delivery System for Lung Cancer Gene Therapy. *Pharmaceutical development and technology* **2016**, *21* (3), 277–281. https://doi.org/10.3109/10837450.2014.996900.

(9) Xie, S.; Yang, F.; Tao, Y.; Chen, D.; Qu, W.; Huang, L.; Liu, Z.; Pan, Y.; Yuan, Z. Enhanced Intracellular Delivery and Antibacterial Efficacy of Enrofloxacin-Loaded Docosanoic Acid Solid Lipid Nanoparticles against Intracellular Salmonella. *Scientific Reports* **2017**, *7* (1), 41104. https://doi.org/10.1038/srep41104.

(10) Smith, T.; Affram, K.; Nottingham, E. L.; Han, B.; Amissah, F.; Krishnan, S.; Trevino, J.; Agyare, E. Application of Smart Solid Lipid Nanoparticles to Enhance the Efficacy of 5-Fluorouracil in the Treatment of Colorectal Cancer. *Scientific Reports* **2020**, *10* (1), 16989. https://doi.org/10.1038/s41598-020-73218-6.

(11) Yuan, H.; Chen, C.-Y.; Chai, G.; Du, Y.-Z.; Hu, F.-Q. Improved Transport and Absorption through Gastrointestinal Tract by PEGylated Solid Lipid Nanoparticles.

Molecular Pharmaceutics **2013**, *10* (5), 1865–1873. https://doi.org/10.1021/mp300649z.

(12) Sadegh Malvajerd, S.; Azadi, A.; Izadi, Z.; Kurd, M.; Dara, T.; Dibaei, M.; Sharif Zadeh, M.; Akbari Javar, H.; Hamidi, M. Brain Delivery of Curcumin Using Solid Lipid Nanoparticles and Nanostructured Lipid Carriers: Preparation, Optimization, and Pharmacokinetic Evaluation. *ACS Chemical Neuroscience* **2019**, *10* (1), 728–739. https://doi.org/10.1021/acschemneuro.8b00510.

(13) Tenchov, R.; Bird, R.; Curtze, A. E.; Zhou, Q. Lipid Nanoparticles—From Liposomes to MRNA Vaccine Delivery, a Landscape of Research Diversity and Advancement. *ACS Nano* **2021**. https://doi.org/10.1021/acsnano.1c04996.

(14) Chariou, P. L.; Ortega-Rivera, O. A.; Steinmetz, N. F. Nanocarriers for the Delivery of Medical, Veterinary, and Agricultural Active Ingredients. *ACS Nano* **2020**, *14* (3), 2678–2701. https://doi.org/10.1021/acsnano.0c00173.

(15) Akbari, V.; Abedi, D.; Pardakhty, A.; Sadeghi-Aliabadi, H. Ciprofloxacin Nano-Niosomes for Targeting Intracellular Infections: An in Vitro Evaluation. *Journal of Nanoparticle Research* **2013**, *15* (4), 1556. https://doi.org/10.1007/s11051-013-1556-y.

(16) Kang, M. H.; Yoo, H. J.; Kwon, Y. H.; Yoon, H. Y.; Lee, S. G.; Kim, S. R.; Yeom, D. W.; Kang, M. J.; Choi, Y. W. Design of Multifunctional Liposomal Nanocarriers for Folate Receptor-Specific Intracellular Drug Delivery. *Molecular Pharmaceutics* **2015**, *12* (12), 4200–4213. https://doi.org/10.1021/acs.molpharmaceut.5b00399.

(17) Afify, M.; Kamel, R. R.; Elhosary, Y. A.; Hegazy, A. E.; Fahim, H. H.; Ezzat, W. M. The Possible Role of Cytochrome c and Programmed Cell Death Protein 4

(PDCD4) on Pathogenesis of Hepatocellular Carcinoma. *Journal of Genetic Engineering and Biotechnology* **2015**, *13* (2), 157–163. https://doi.org/https://doi.org/10.1016/j.jgeb.2015.10.002.

(18) Vladimirov, Y.; Nol, Y.; Volkov, V. Protein-Lipid-Nanoparticles That Determine Whether Cells Will Live or Die. *Crystallography Reports - CRYSTALLOGR REP* **2011**, *56*, 553–559. https://doi.org/10.1134/S1063774511040250.

(19) Vladimirov, G. K.; Remenshchikov, V. E.; Nesterova, A. M.; Volkov, V. v; Vladimirov, Y. A. Comparison of the Size and Properties of the Cytochrome c/Cardiolipin Nanospheres in a Sediment and Non-Polar Medium. *Biochemistry (Moscow)*. Pleiades Publishing: Moscow 2019, pp 923–930. https://doi.org/10.1134/S000629791908008X.

(20) Li, M.; Mandal, A.; Tyurin, V. A.; DeLucia, M.; Ahn, J.; Kagan, V. E.; van der Wel, P. C. A. Surface-Binding to Cardiolipin Nanodomains Triggers Cytochrome c Pro-Apoptotic Peroxidase Activity via Localized Dynamics. *Structure* **2019**, *27* (5), 806-815.e4. https://doi.org/https://doi.org/10.1016/j.str.2019.02.007.

(21) Vladimirov, Y.; Proskurnina, E.; Izmailov, D.; Novikov, A.; Brusnichkin, A.; Osipov, A.; Kagan, V. Cardiolipin Activates Cytochrome c Peroxidase Activity since It Facilitates H2O2 Access to Heme. *Biochemistry. Biokhimiia* **2006**, *71*, 998–1005. https://doi.org/10.1134/S0006297906090082.

(22) Vladimirov, Y.; Proskurnina, E.; Alekseev, A. Molecular Mechanisms of Apoptosis. Structure of Cytochrome c-Cardiolipin Complex. *Biochemistry. Biokhimiia* **2013**, *78*, 1086–1097. https://doi.org/10.1134/S0006297913100027.

(23) Brown, L. R.; Wüthrich, K. NMR and ESR Studies of the Interactions of Cytochrome c with Mixed Cardiolipin-Phosphatidylcholine Vesicles. *Biochimica et Biophysica Acta (BBA) - Biomembranes* **1977**, *468* (3), 389–410. https://doi.org/https://doi.org/10.1016/0005-2736(77)90290-5.

(24) Mikhailov, V.; Mikhailova, M.; Degenhardt, K.; Venkatachalam, M. A.; White, E.; Saikumar, P. Association of Bax and Bak Homo-Oligomers in Mitochondria: Bax REQUIREMENT FOR Bak REORGANIZATION AND CYTOCHROMEc RELEASE*. *Journal of Biological Chemistry* **2003**, *278* (7), 5367–5376. https://doi.org/https://doi.org/10.1074/jbc.M203392200.

(25) Große, L.; Wurm, C. A.; Brüser, C.; Neumann, D.; Jans, D. C.; Jakobs, S. Bax Assembles into Large Ring-like Structures Remodeling the Mitochondrial Outer Membrane in Apoptosis. *The EMBO Journal* **2016**, *35* (4), 402–413. https://doi.org/https://doi.org/10.15252/embj.201592789.

(26) Ott, M.; Robertson, J.; Gogvadze, V.; Zhivotovsky, B.; Orrenius, S. Cytochrome c Release from Mitochondria Proceeds by a Two-Step Process. *Proceedings of the National Academy of Sciences of the United States of America* **2002**, *99*, 1259–1263. https://doi.org/10.1073/pnas.241655498.

(27) Garrido, C.; Galluzzi, L.; Brunet, M.; Puig, P.E.; Didelot, C.; Kroemer, G. Mechanisms of Cytochrome c Release from Mitochondria. *Cell Deat & Differentiation* **2006**, *13* (9), 1423-1433. https://doi.org/10.1038/sj.cdd.4401950.

(28) Vladimirov, G.; Vikulina, A. S.; Volodkin, D. v; Vladimirov, Y. Structure of the Complex of Cytochrome c with Cardiolipin in Non-Polar Environment. *Chemistry*

and Physics of Lipids **2018**, *214*. https://doi.org/10.1016/j.chemphyslip.2018.05.007.

(29) American Cancer Society. Cancer Facts & Figures for Hispanics/Latinos 2018-2020. American Cancer Society, Inc.: Atlanta 2018.

(30) Vladimirov, Y.; Sarisozen, C.; Vladimirov, G.; Filipczak, N.; Nesterova, A.; Torchilin, V. The Cytotoxic Action of Cytochrome C/Cardiolipin Nanocomplex (Cyt-CL) on Cancer Cells in Culture. *Pharmaceutical Research* **2017**, *34*. https://doi.org/10.1007/s11095-017-2143-1.

(31) Symons, J. L.; Cho, K.-J.; Chang, J. T.; Du, G.; Waxham, M. N.; Hancock, J. F.; Levental, I.; Levental, K. R. Lipidomic Atlas of Mammalian Cell Membranes Reveals Hierarchical Variation Induced by Culture Conditions, Subcellular Membranes, and Cell Lineages. *Soft Matter* **2021**, *17* (2), 288–297. https://doi.org/10.1039/D0SM00404A.

(32) Sharifian Gh., M. Recent Experimental Developments in Studying Passive Membrane Transport of Drug Molecules. *Molecular Pharmaceutics* **2021**, *18* (6), 2122–2141. https://doi.org/10.1021/acs.molpharmaceut.1c00009.

(33) Kobayashi, T.; Menon, A. K. Transbilayer Lipid Asymmetry. *Current Biology* **2018**, *28* (8), R386–R391. https://doi.org/https://doi.org/10.1016/j.cub.2018.01.007.

(34) Luchini, A.; Vitiello, G. Mimicking the Mammalian Plasma Membrane: An Overview of Lipid Membrane Models for Biophysical Studies. *Biomimetics* **2021**, *6* (1). https://doi.org/10.3390/biomimetics6010003.

(35) Lundbæk, J. A.; Collingwood, S. A.; Ingólfsson, H. I.; Kapoor, R.; Andersen, O. S. Lipid Bilayer Regulation of Membrane Protein Function: Gramicidin Channels as

Molecular Force Probes. *Journal of The Royal Society Interface* **2010**, *7* (44), 373–395. https://doi.org/10.1098/rsif.2009.0443.

(36) Yang, N. J.; Hinner, M. J. Getting across the Cell Membrane: An Overview for Small Molecules, Peptides, and Proteins. *Methods in molecular biology (Clifton, N.J.)* **2015**, *1266*, 29–53. https://doi.org/10.1007/978-1-4939-2272-7_3.

(37) Schenkel, L. C.; Bakovic, M. Formation and Regulation of Mitochondrial Membranes. *International journal of cell biology* **2014**, *2014*, 709828. https://doi.org/10.1155/2014/709828.

(38) Keenan, S.; Watt, M.; Montgomery, M. Inter-Organelle Communication in the Pathogenesis of Mitochondrial Dysfunction and Insulin Resistance. *Current Diabetes Reports* **2020**, *20*. https://doi.org/10.1007/s11892-020-01300-4.

(39) Lewis, R. N. A. H.; McElhaney, R. N. The Physicochemical Properties of Cardiolipin Bilayers and Cardiolipin-Containing Lipid Membranes. *Biochimica et Biophysica Acta (BBA) - Biomembranes* **2009**, *1788* (10), 2069–2079. https://doi.org/https://doi.org/10.1016/j.bbamem.2009.03.014.

(40) Luchini, A.; Cavasso, D.; Radulescu, A.; D'Errico, G.; Paduano, L.; Vitiello, G. Structural Organization of Cardiolipin-Containing Vesicles as Models of the Bacterial Cytoplasmic Membrane. *Langmuir* **2021**, *37* (28), 8508–8516. https://doi.org/10.1021/acs.langmuir.1c00981.

(41) Phan, H. T.; Haes, A. J. What Does Nanoparticle Stability Mean? *The Journal of Physical Chemistry C* **2019**, *123* (27), 16495–16507. https://doi.org/10.1021/acs.jpcc.9b00913.

(42) Danaei, M.; Dehghankhold, M.; Ataei, S.; Hasanzadeh Davarani, F.; Javanmard, R.; Dokhani, A.; Khorasani, S.; Mozafari, M. R. Impact of Particle Size and Polydispersity Index on the Clinical Applications of Lipidic Nanocarrier Systems. *Pharmaceutics* **2018**, *10* (2). https://doi.org/10.3390/pharmaceutics10020057.

(43) Piroeva, I.; Atanassova-Vladimirova, S.; Dimowa, L.; Sbirkova, H.; Radoslavov, G.; Hristov, P.; Shivachev, B. L. A Simple and Rapid Scanning Electron Microscope Preparative Technique for Observation of Biological Samples: Application on Bacteria and DNA Samples. *Bulg. Chem. Commun.* **2013**, *45* (4), 510-515. Vol. 45. https://doi.org/10.1002/jemt.10184

(44) Alexandri, E., Ahmed, R., Siddiqui, H., Choudhary, M. I., Tsiafoulis, C. G., & Gerothanassis, I. P. High Resolution NMR Spectroscopy as a Structural and Analytical Tool for Unsaturated Lipids in Solution. *Molecules* **2017**, *22*(10). https://doi.org/10.3390/molecules22101663

Appendix A

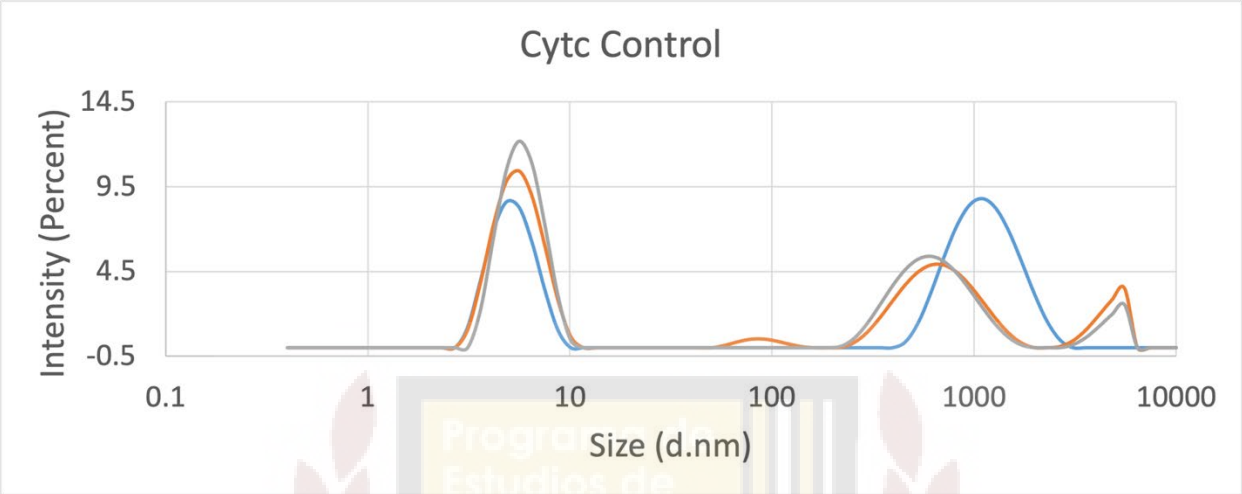

Figure S1: Size Distribution by Intensity for Cytc control solution

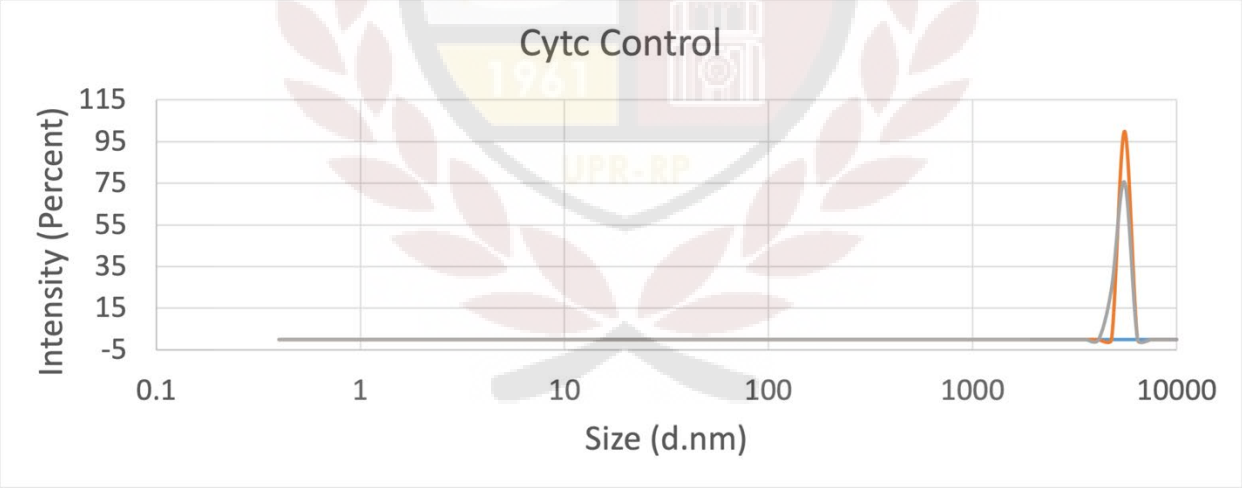

Figure S2: Size Distribution by Intensity for Cytc control solution after centrifugation

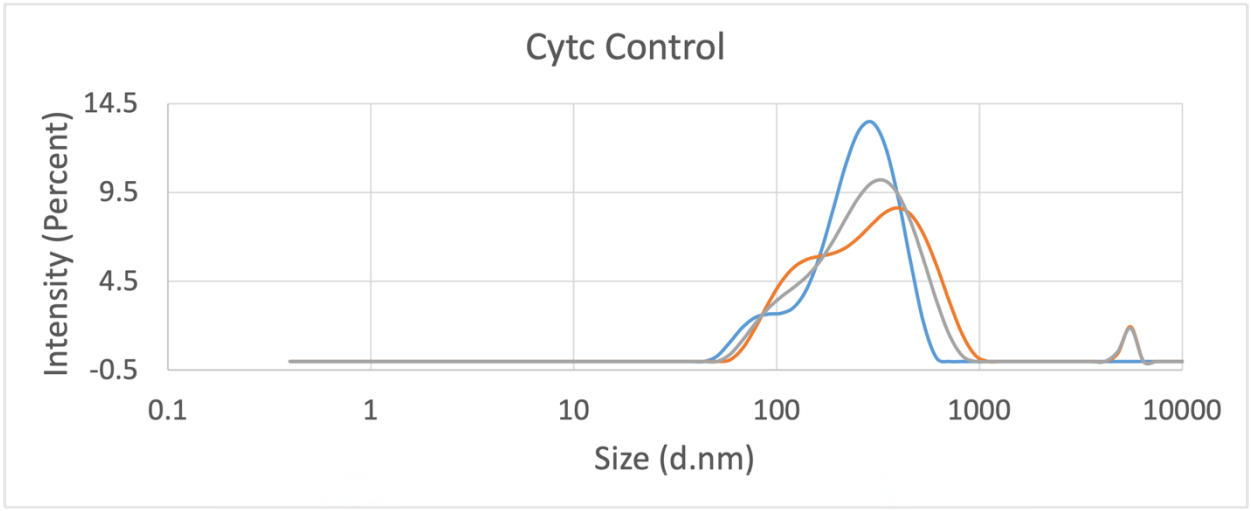

Figure S3: Size Distribution by Intensity for Cytc control solution after centrifugation and extrusion

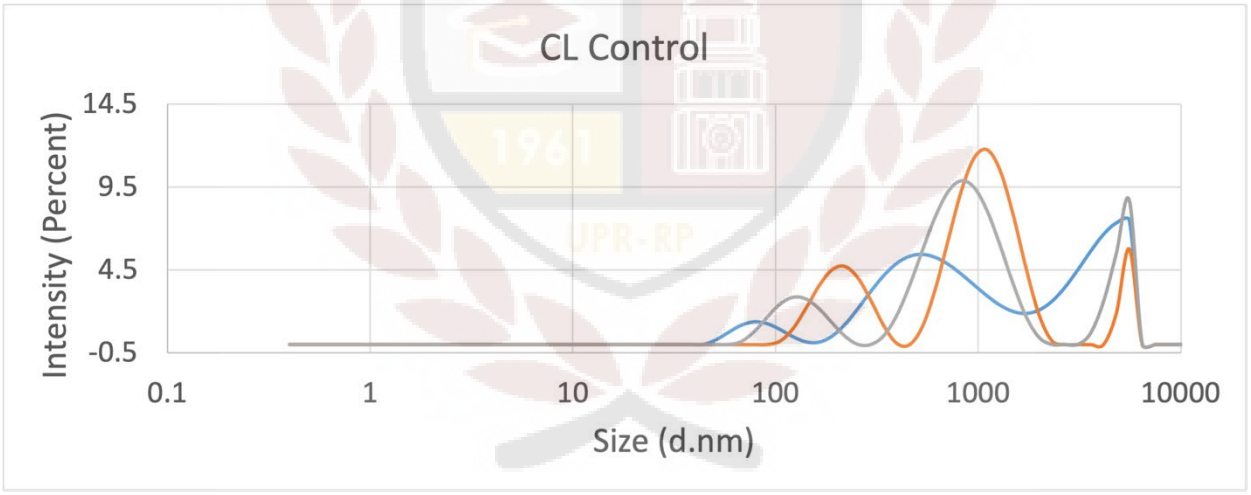

Figure S4: Size Distribution by Intensity for CL control solution

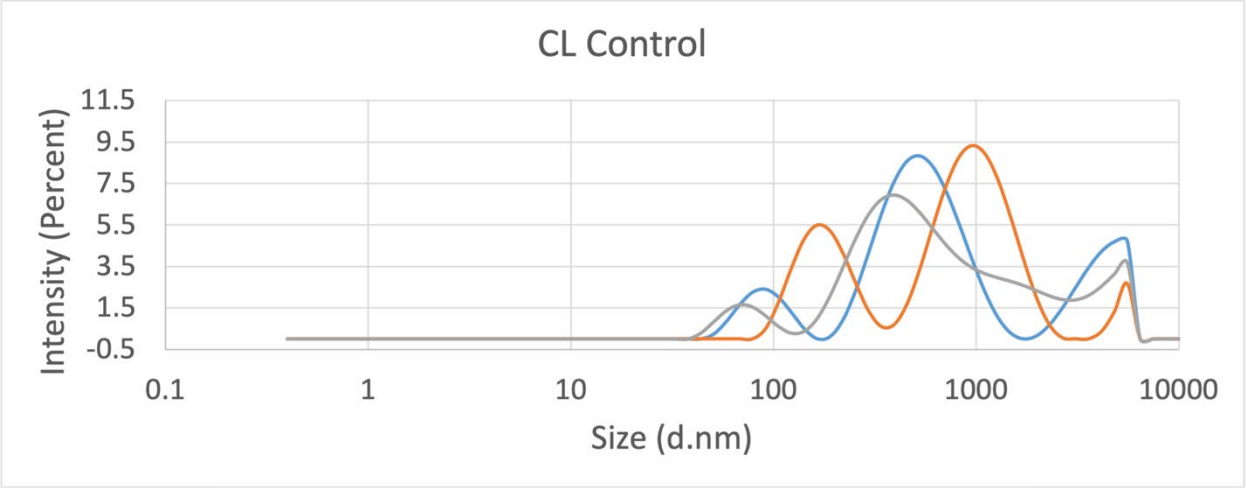

Figure S5: Size Distribution by Intensity for CL control solution after centrifugation

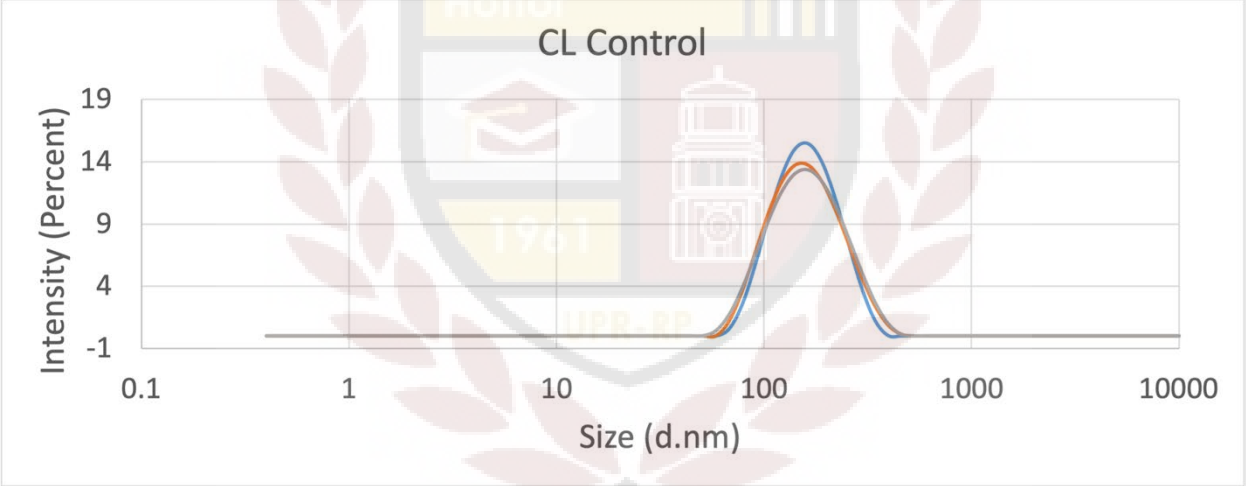

Figure S6: Size Distribution by Intensity for CL control solution after centrifugation and extrusion

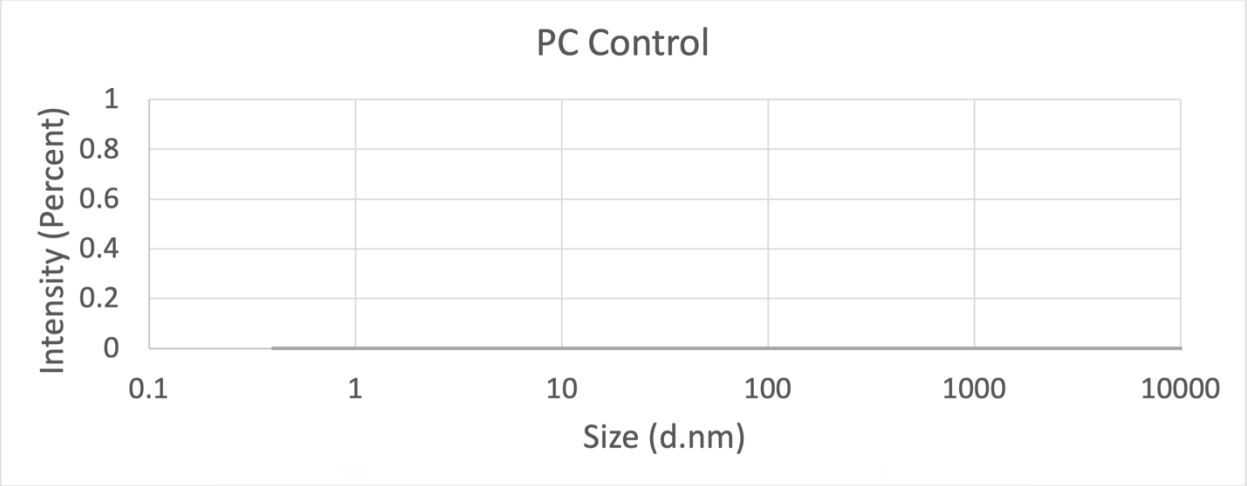

Figure S7: Size Distribution by Intensity for PC control solution

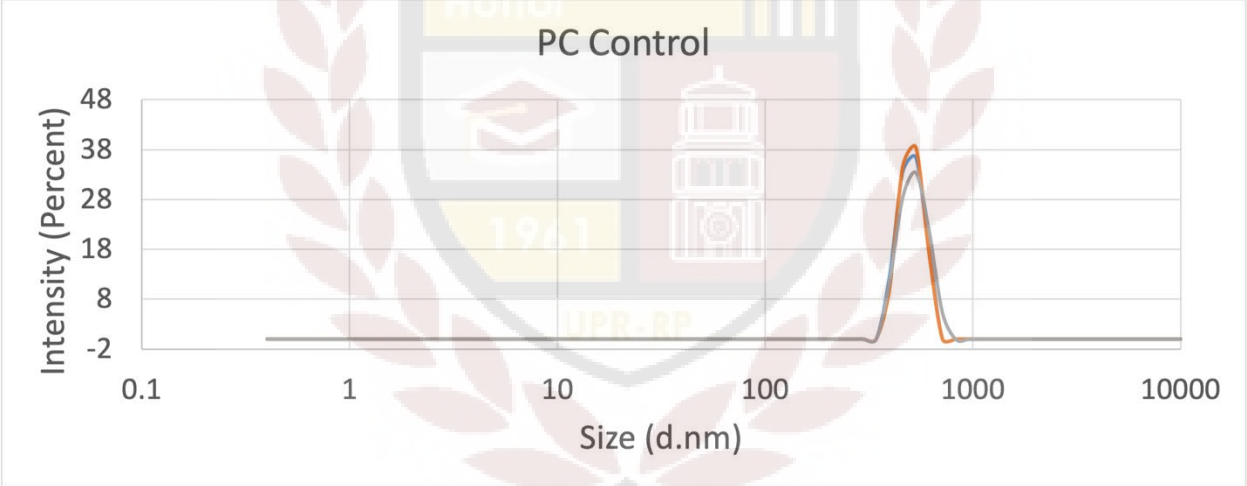

Figure S8: Size Distribution by Intensity for PC control solution after centrifugation

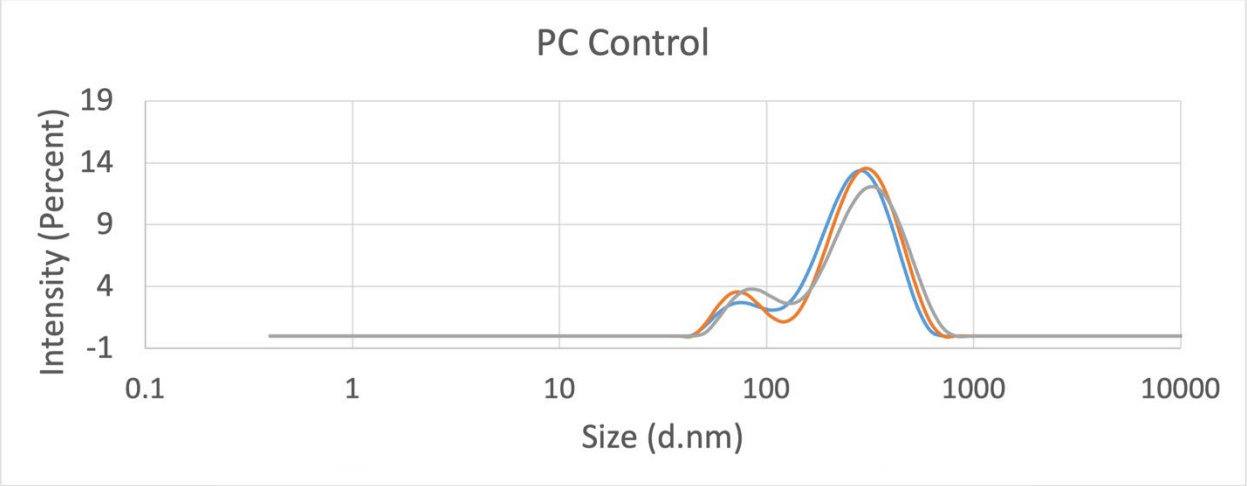

Figure S9: Size Distribution by Intensity for PC control solution after centrifugation and extrusion

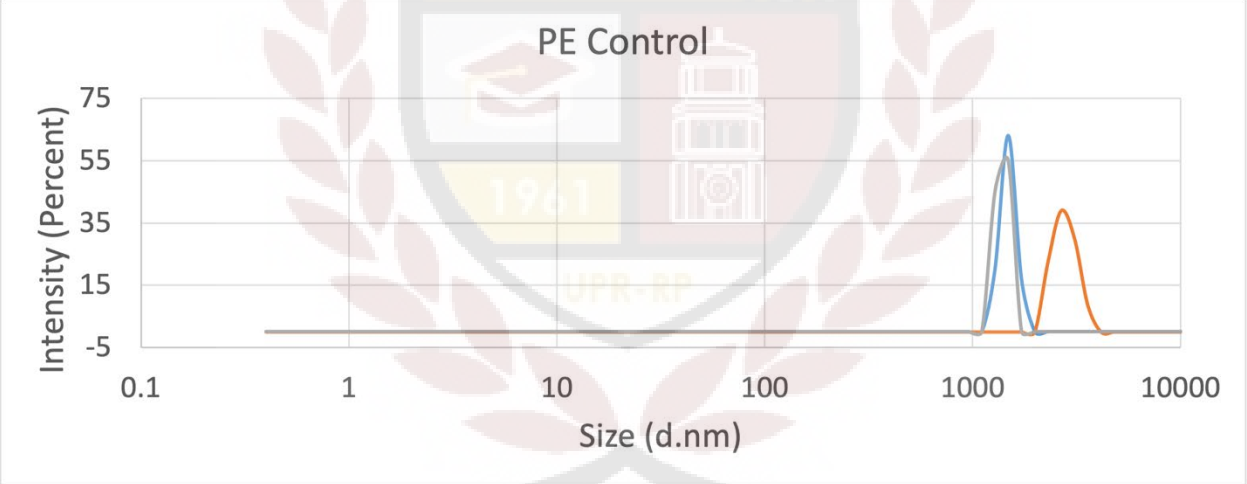

Figure S10: Size Distribution by Intensity for PE control solution

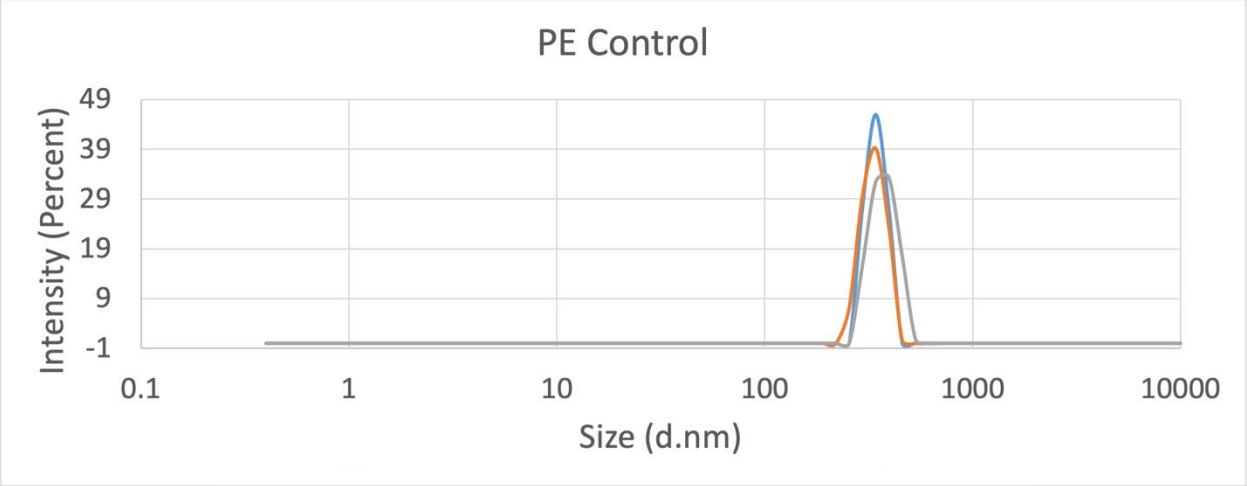

Figure S11: Size Distribution by Intensity for PE control solution after centrifugation

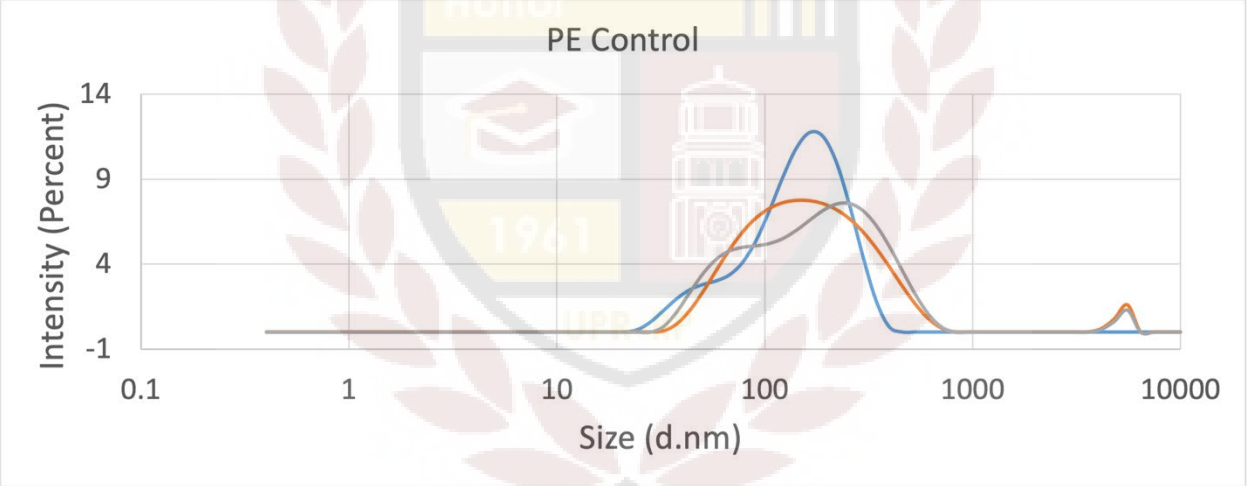

Figure S12: Size Distribution by Intensity for PE control solution after centrifugation and extrusion

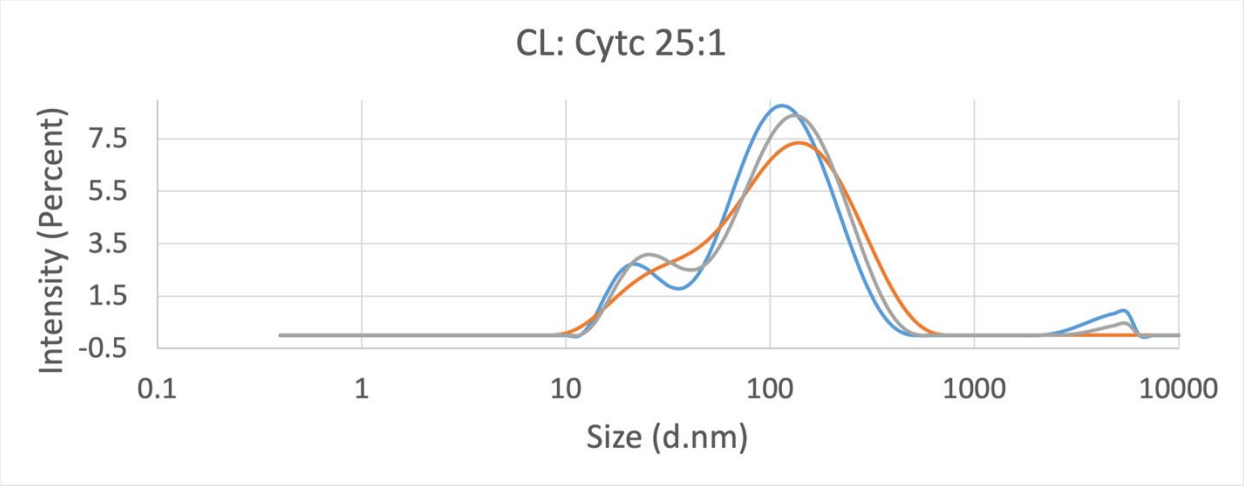

Figure S13: Size Distribution by Intensity for CL: Cytc 25:1 nanoparticle solution

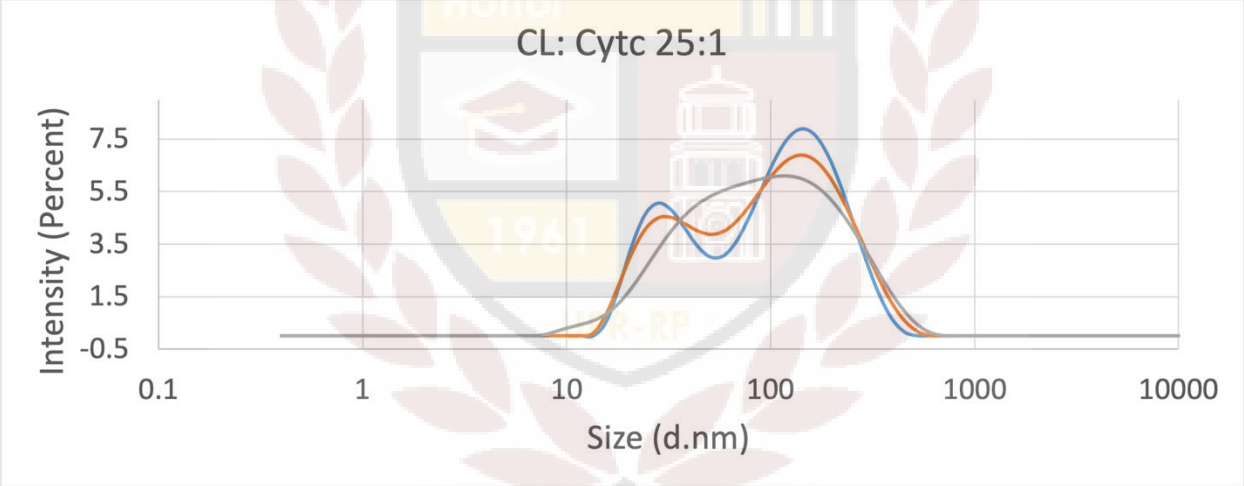

Figure S14: Size Distribution by Intensity for CL: Cytc 25:1 nanoparticle solution after centrifugation

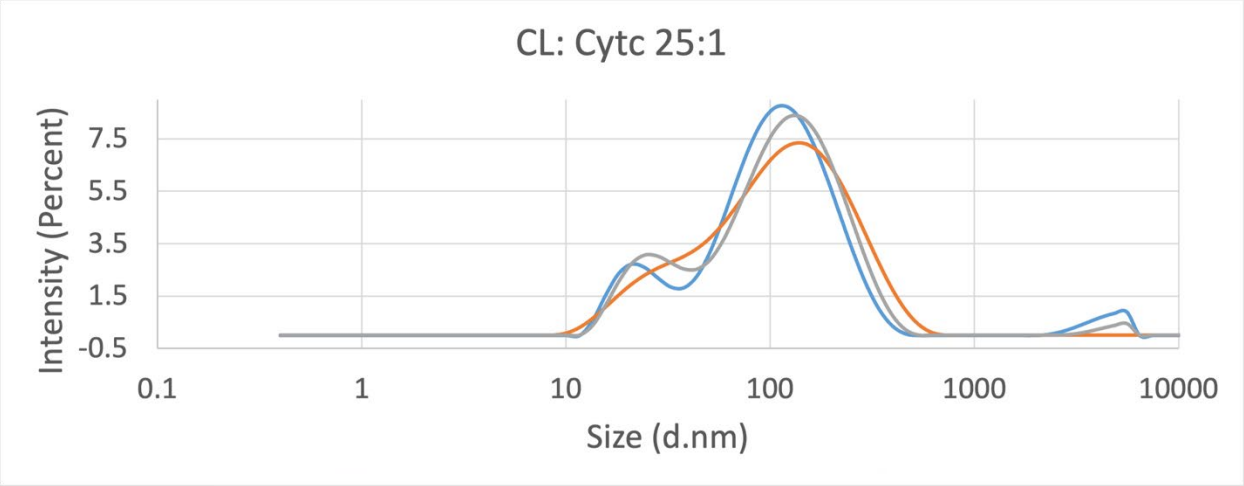

Figure S15: Size Distribution by Intensity for CL: Cytc 25:1 nanoparticle solution after centrifugation and extrusion

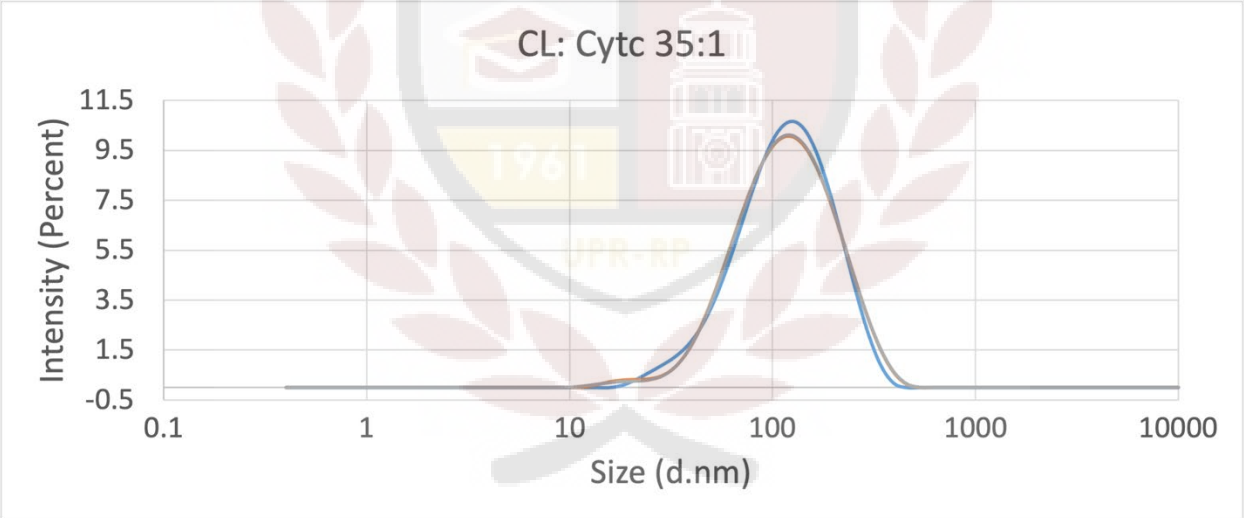

Figure S16: Size Distribution by Intensity for CL: Cytc 35:1 nanoparticle solution

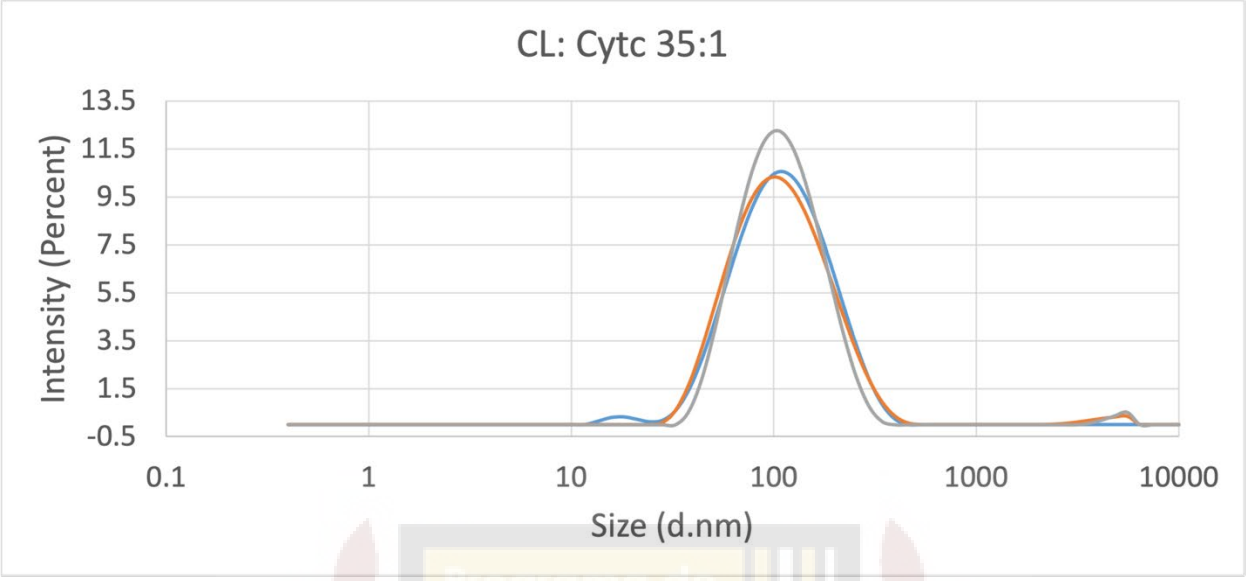

Figure S17: Size Distribution by Intensity for CL: Cytc 35:1 nanoparticle solution after centrifugation

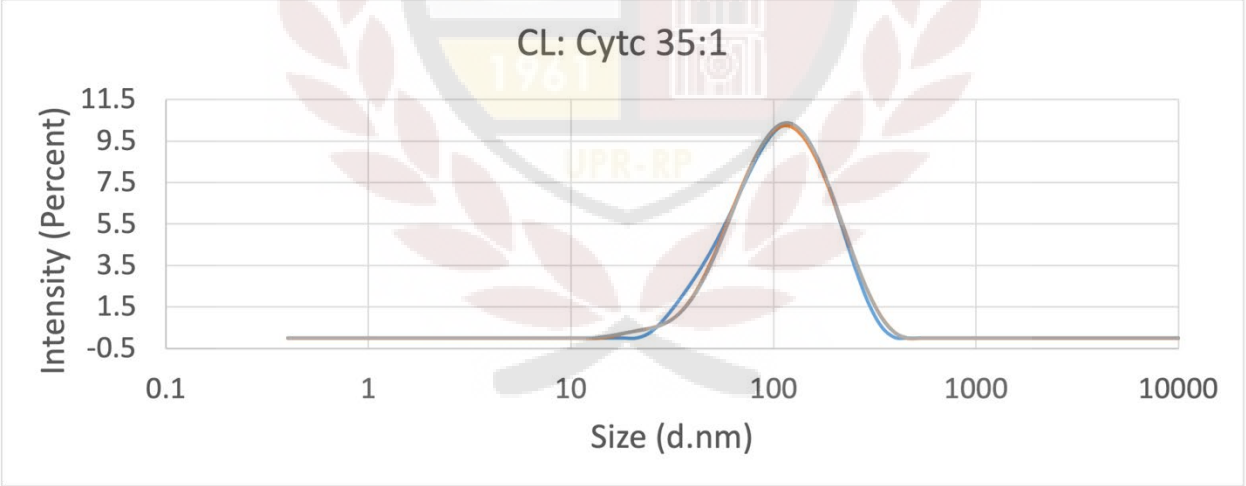

Figure S18: Size Distribution by Intensity for CL: Cytc 35:1 nanoparticle solution after centrifugation and extrusion

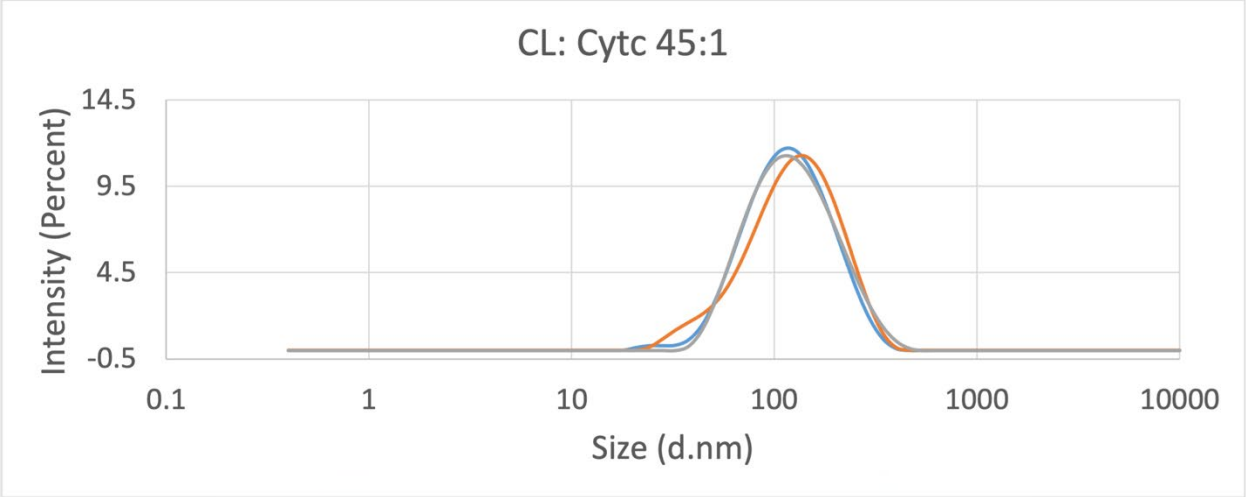

Figure S19: Size Distribution by Intensity for CL: Cytc 45:1 nanoparticle solution

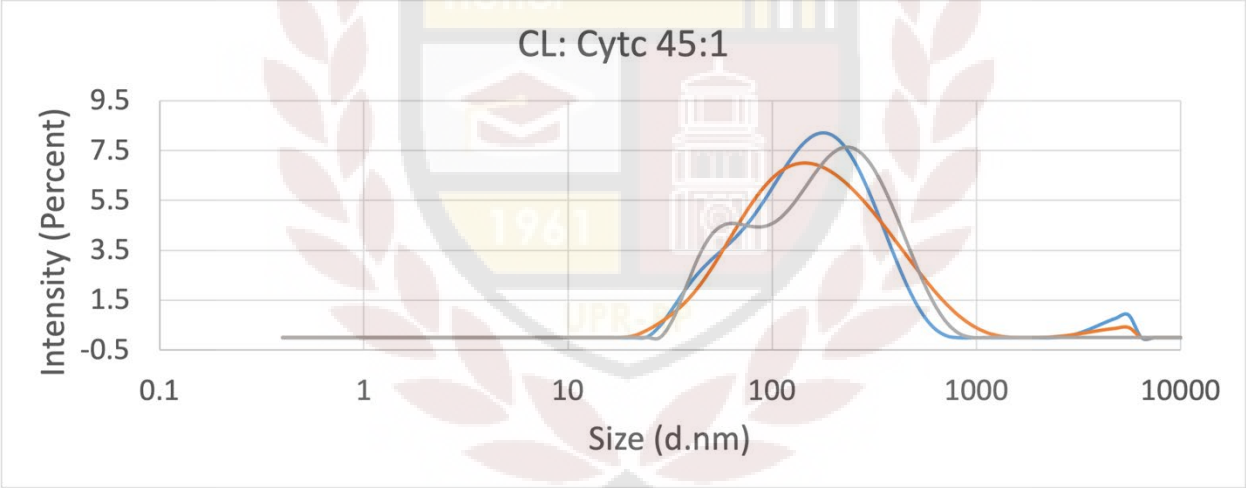

Figure S20: Size Distribution by Intensity for CL: Cytc 45:1 nanoparticle solution after centrifugation

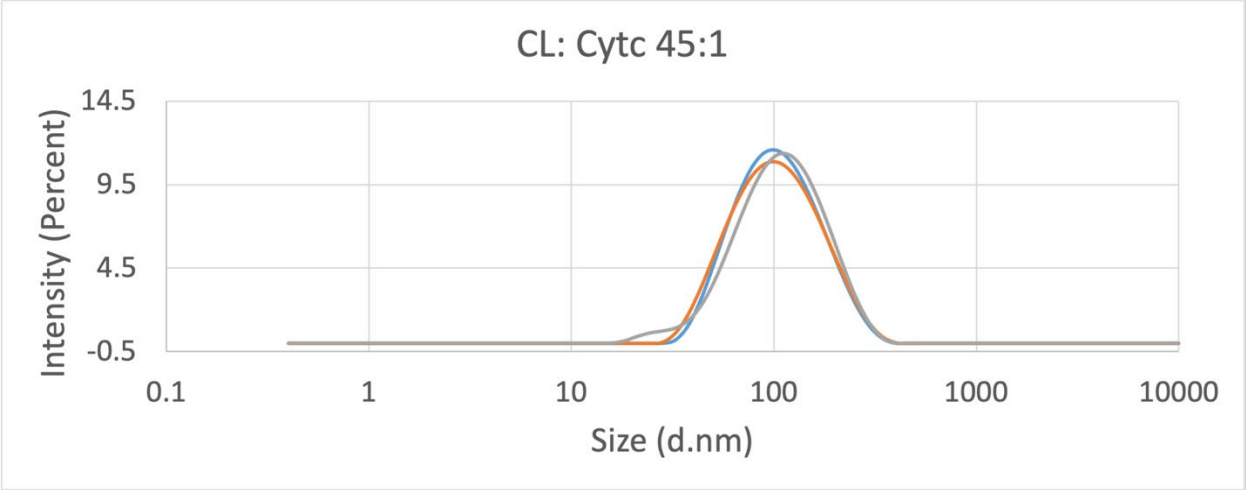

Figure S21: Size Distribution by Intensity for CL: Cytc 45:1 nanoparticle solution after centrifugation and extrusion

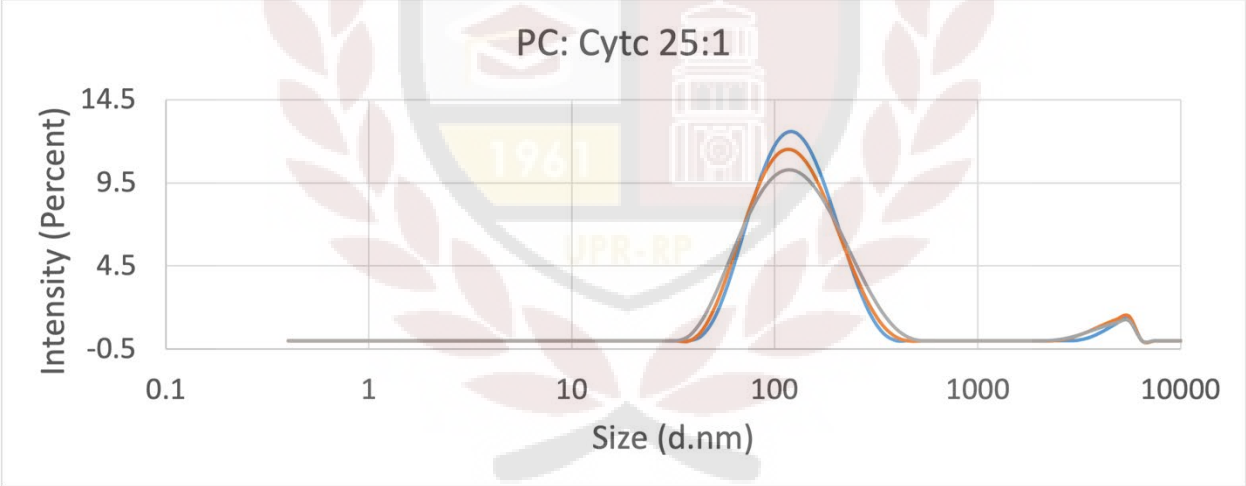

Figure S22: Size Distribution by Intensity for PC: Cytc 25:1 nanoparticle solution

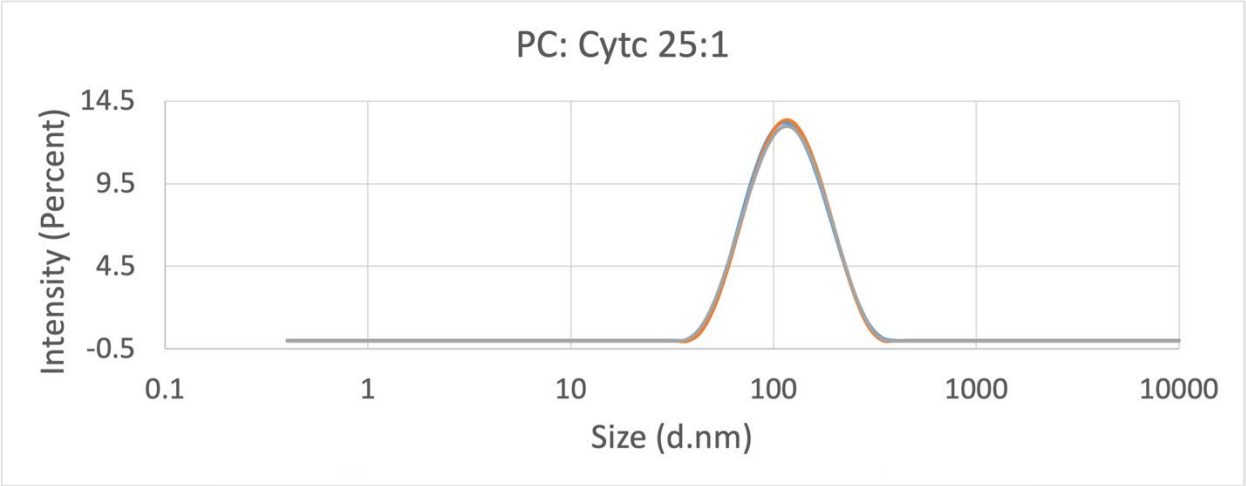

Figure S23: Size Distribution by Intensity for PC: Cytc 25:1 nanoparticle solution after centrifugation

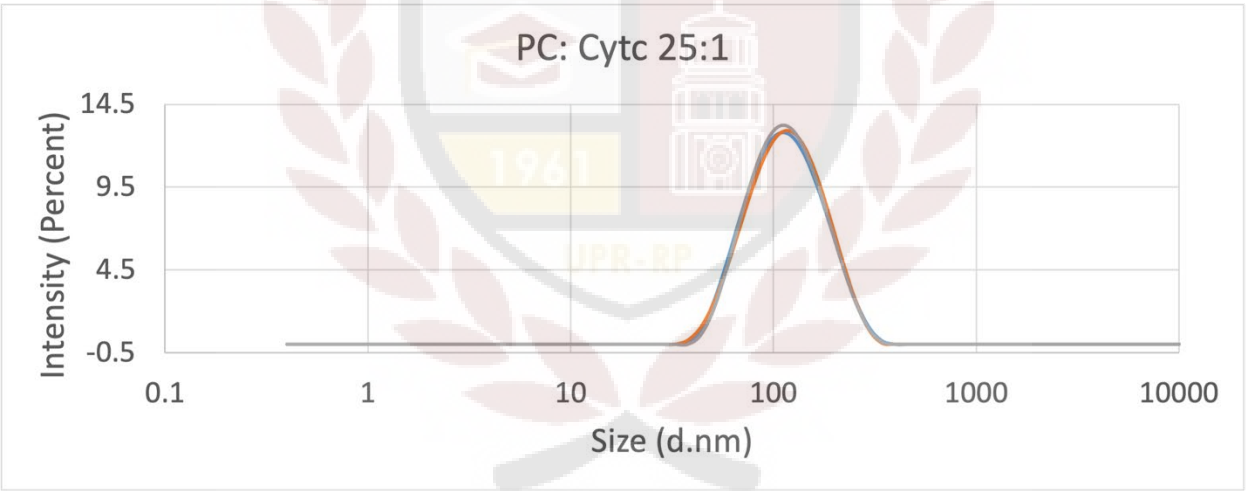

Figure S24: Size Distribution by Intensity for PC: Cytc 25:1 nanoparticle solution after centrifugation and extrusion

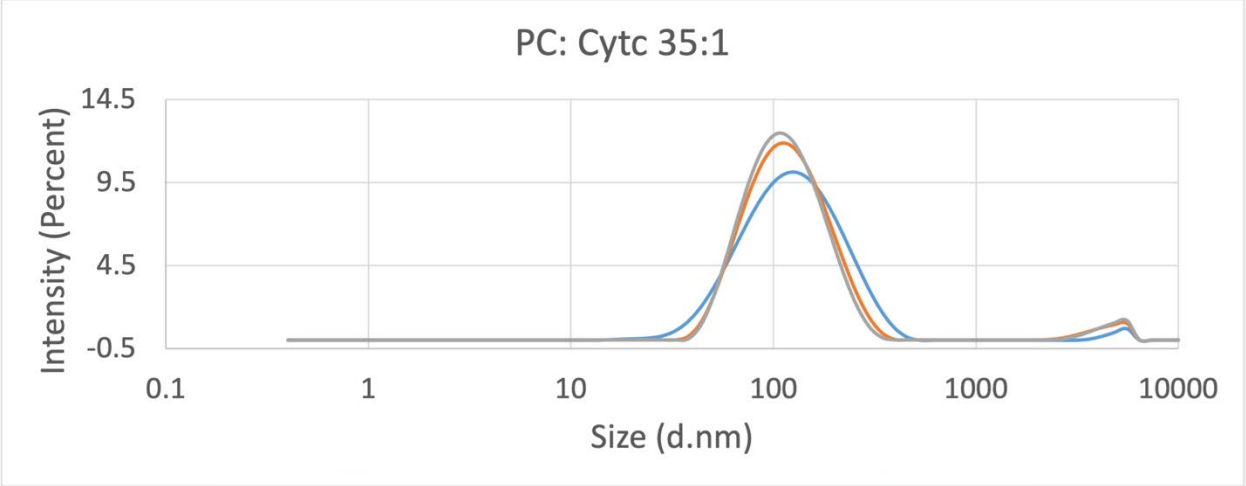

Figure S25: Size Distribution by Intensity for PC: Cytc 35:1 nanoparticle solution

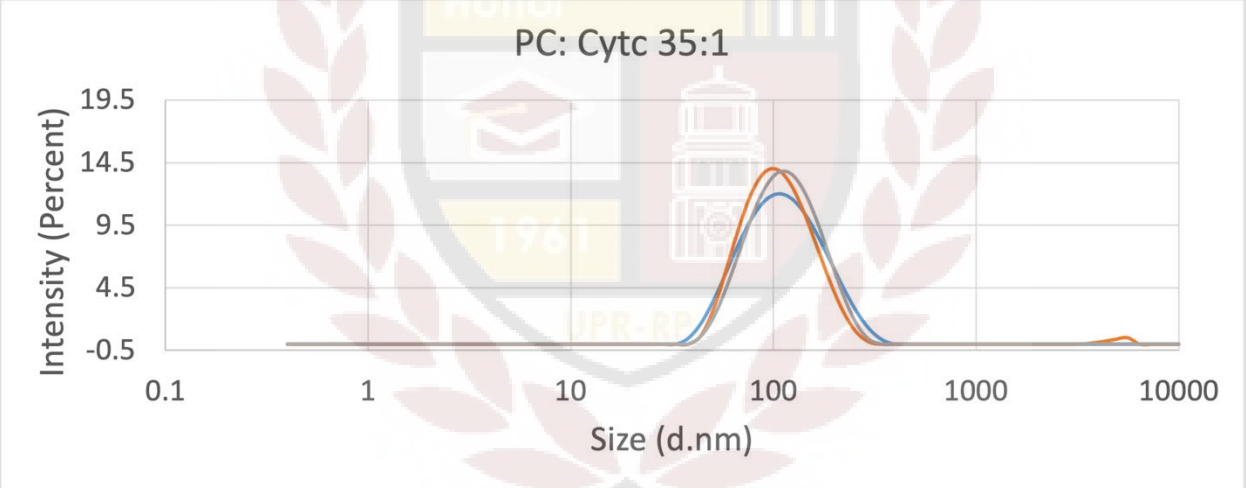

Figure S26: Size Distribution by Intensity for PC: Cytc 35:1 nanoparticle solution after centrifugation

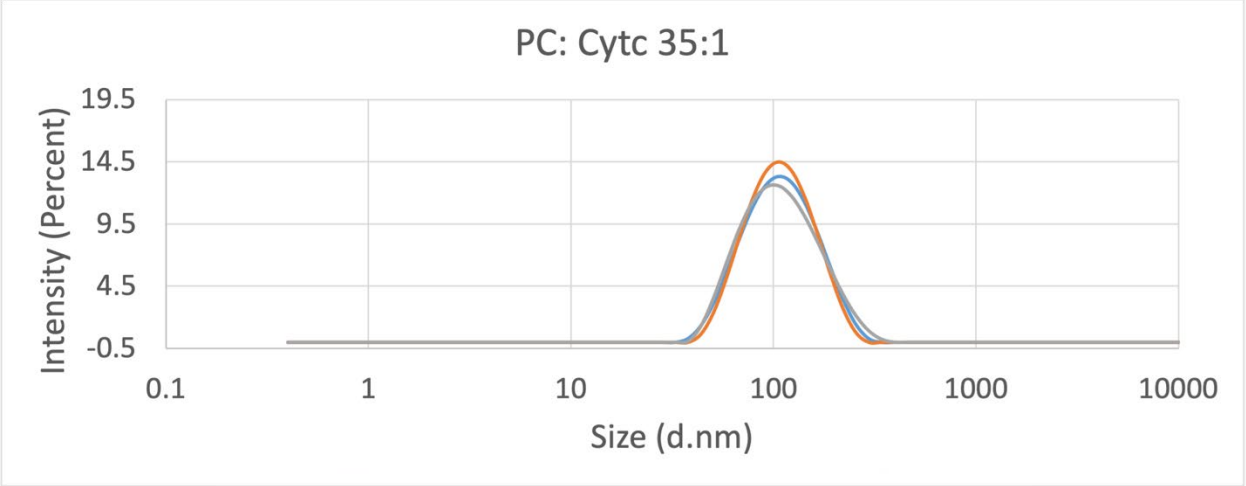

Figure S27: Size Distribution by Intensity for PC: Cytc 35:1 nanoparticle solution after centrifugation and extrusion

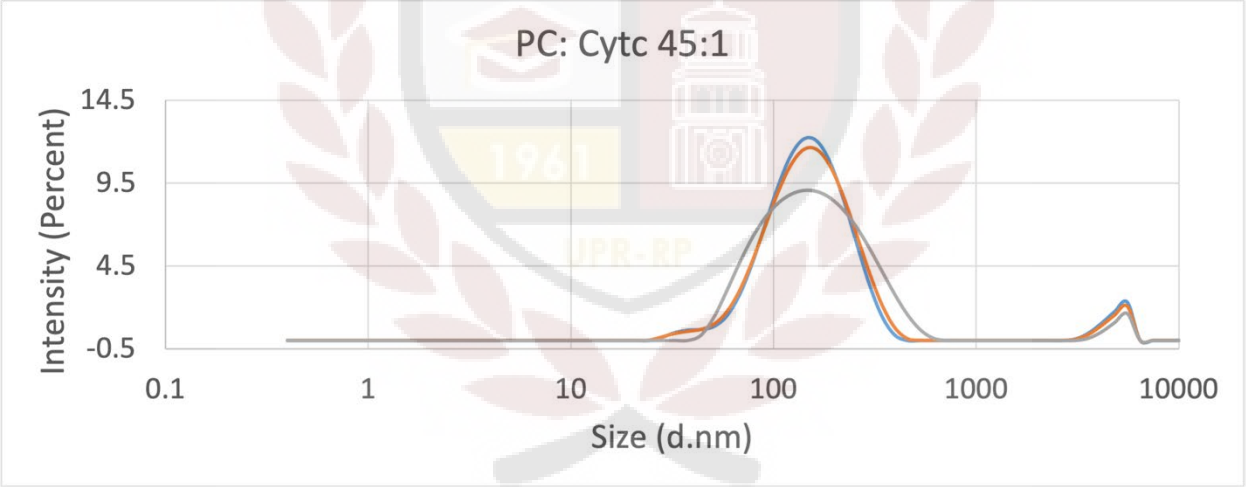

Figure S28: Size Distribution by Intensity for PC: Cytc 45:1 nanoparticle solution

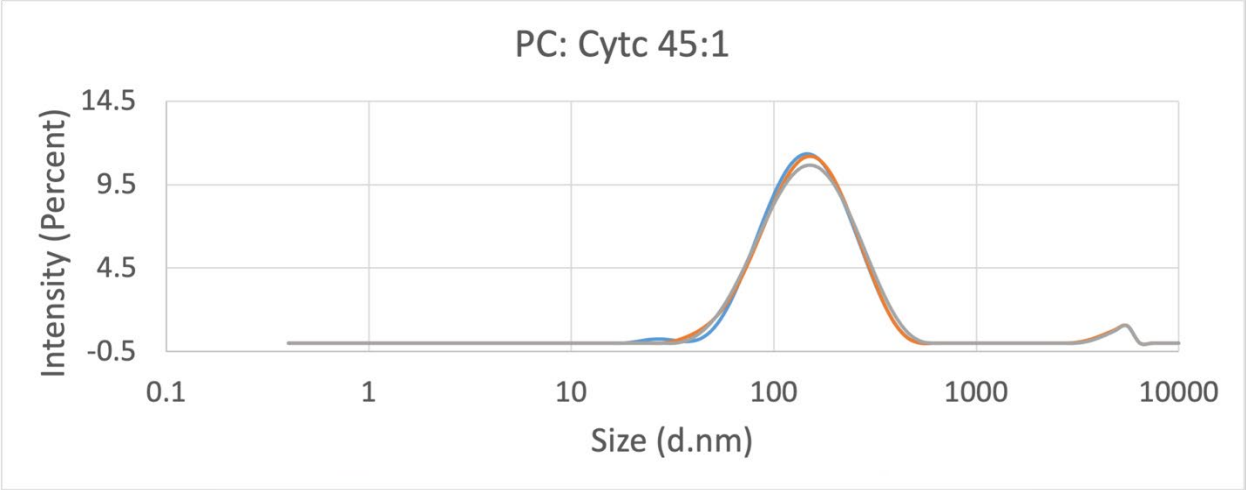

Figure S29: Size Distribution by Intensity for PC: Cytc 45:1 nanoparticle solution after centrifugation

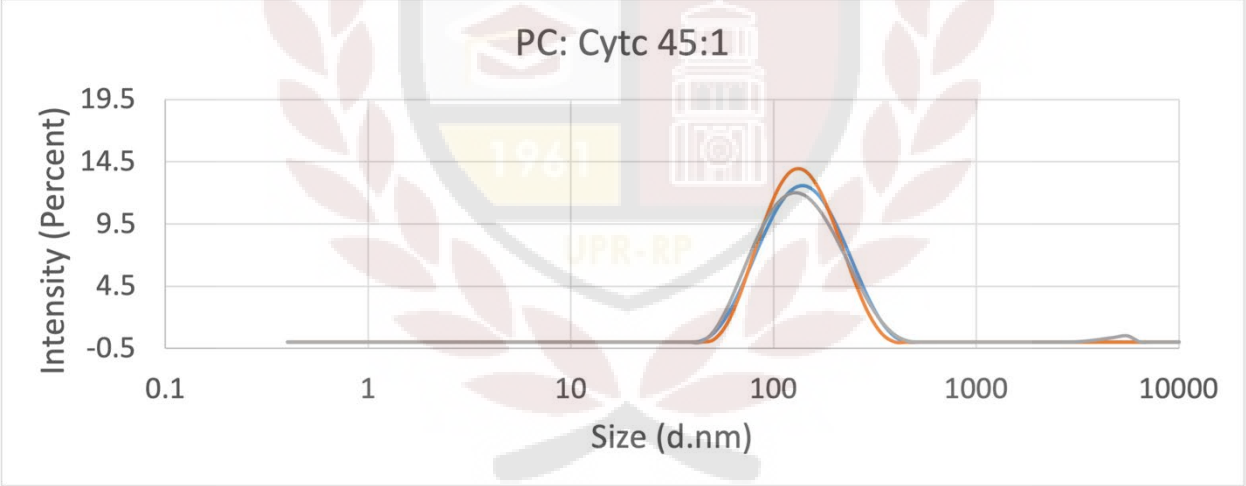

Figure S30: Size Distribution by Intensity for PC: Cytc 45:1 nanoparticle solution after centrifugation and extrusion

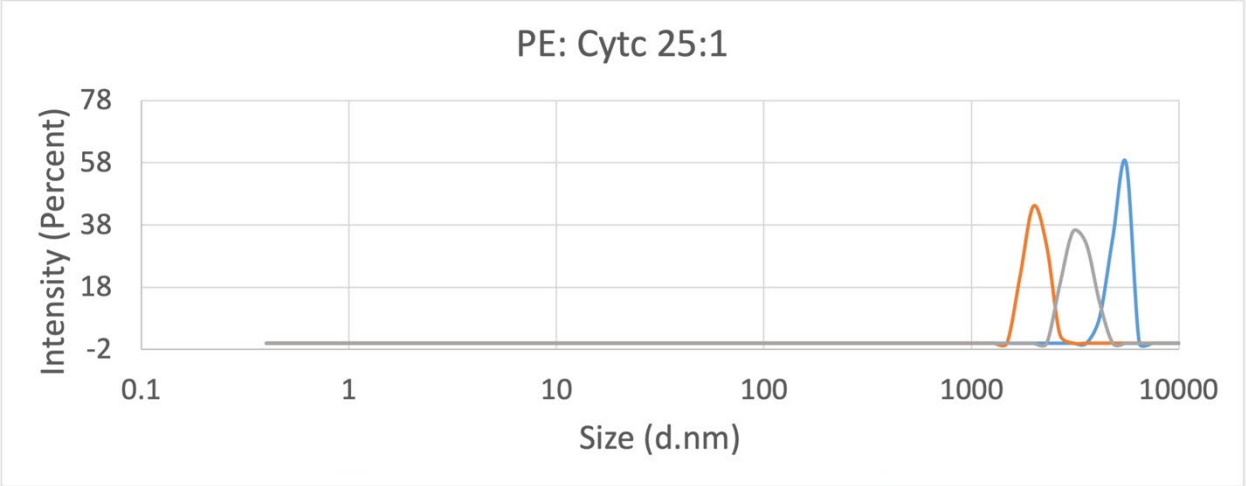

Figure S31: Size Distribution by Intensity for PE: Cytc 25:1 nanoparticle solution

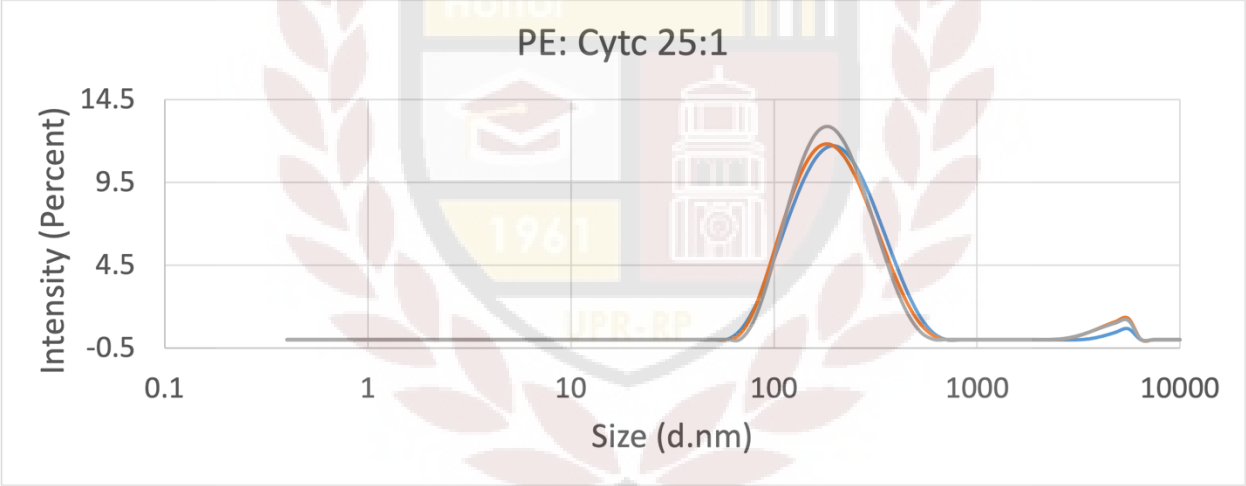

Figure S32: Size Distribution by Intensity for PE: Cytc 25:1 nanoparticle solution after centrifugation

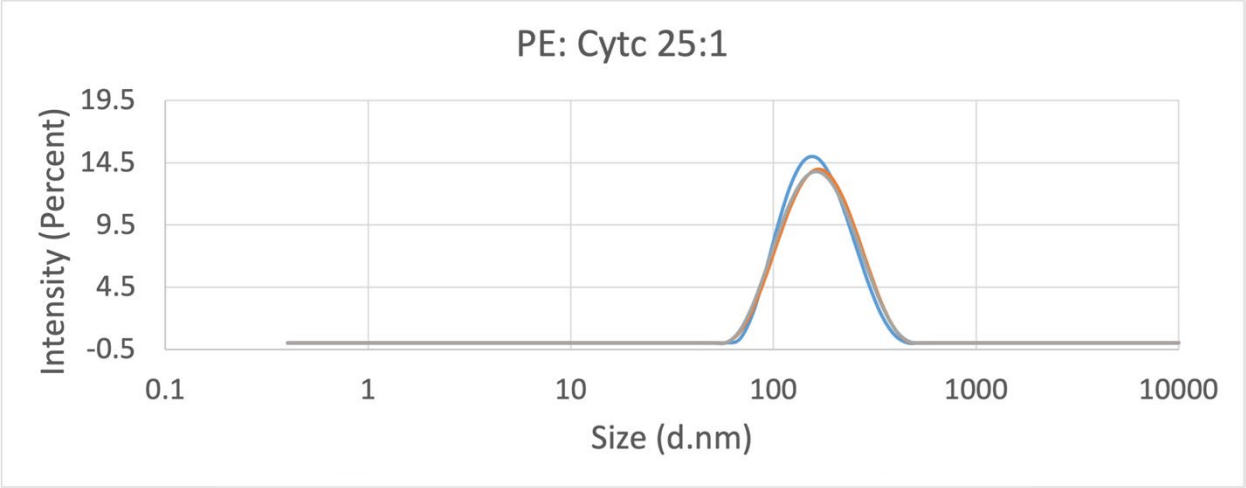

Figure S33: Size Distribution by Intensity for PE: Cytc 25:1 nanoparticle solution after centrifugation and extrusion

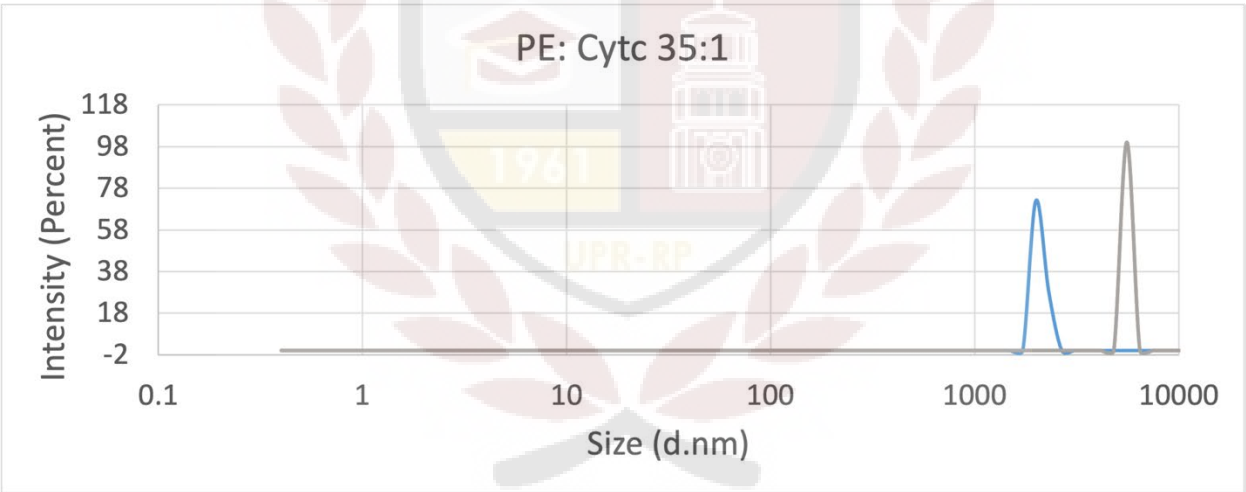

Figure S34: Size Distribution by Intensity for PE: Cytc 35:1 nanoparticle solution

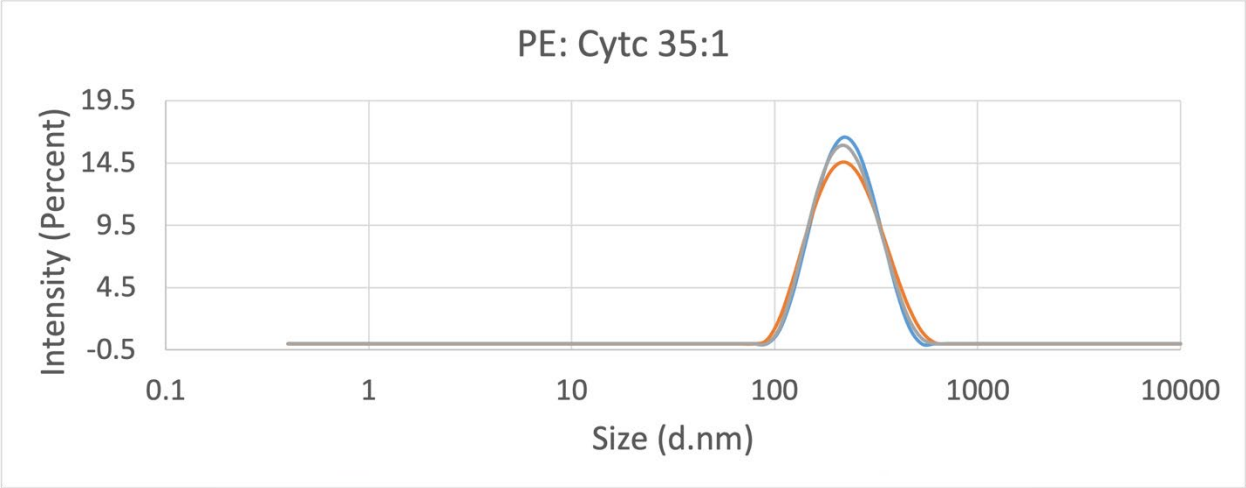

Figure S35: Size Distribution by Intensity for PE: Cytc 35:1 nanoparticle solution after centrifugation

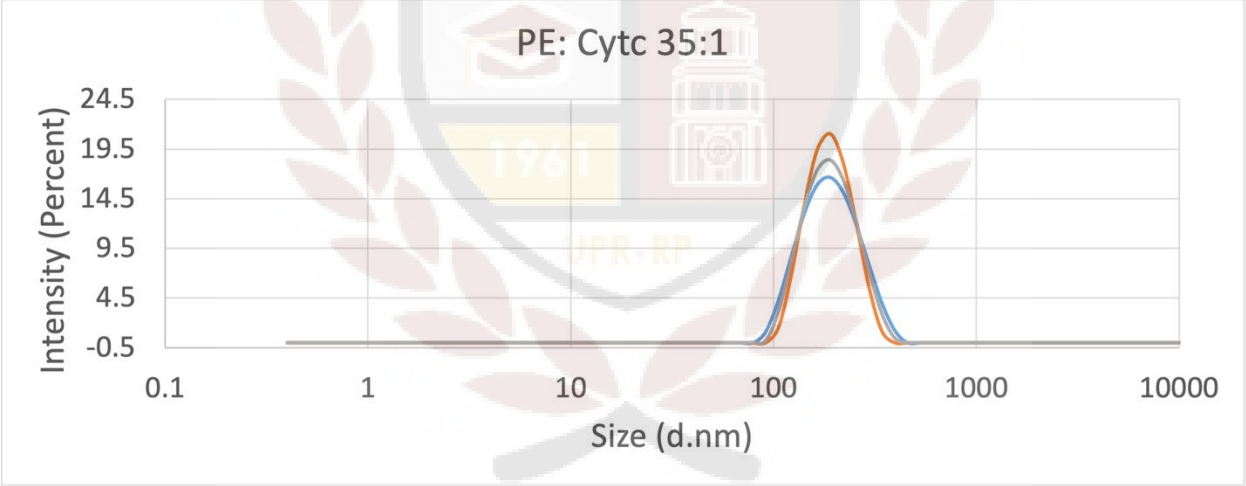

Figure S36: Size Distribution by Intensity for PE: Cytc 35:1 nanoparticle solution after centrifugation and extrusion

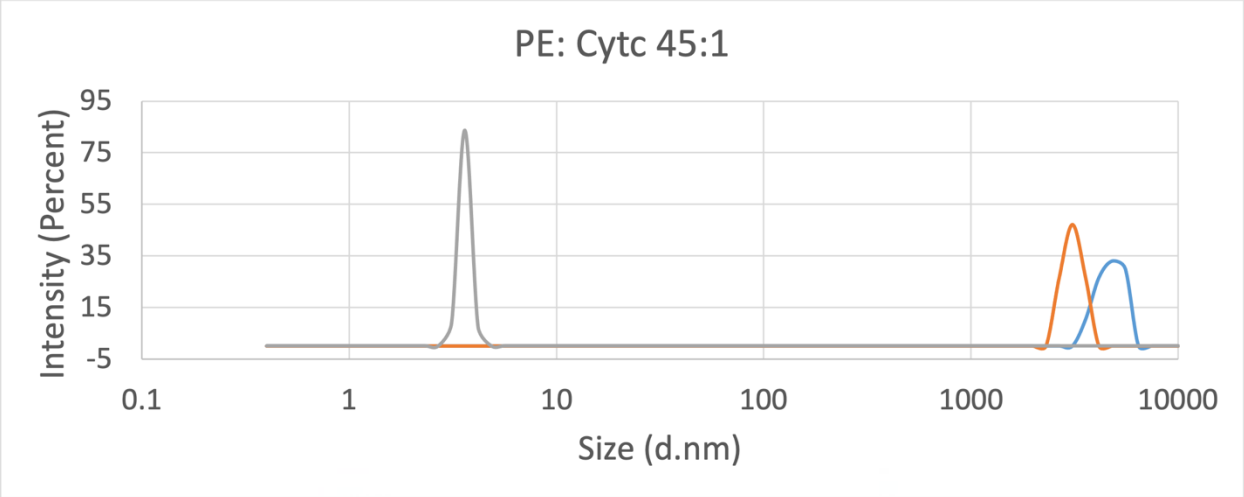

Figure S37: Size Distribution by Intensity for PE: Cytc 45:1 nanoparticle solution

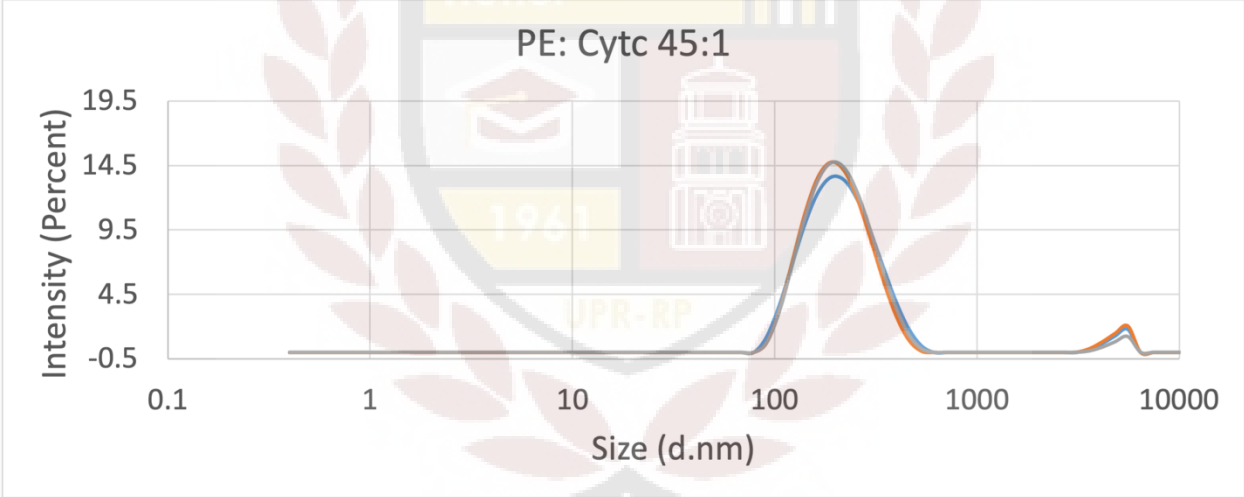

Figure S38: Size Distribution by Intensity for PE: Cytc 45:1 nanoparticle solution after centrifugation

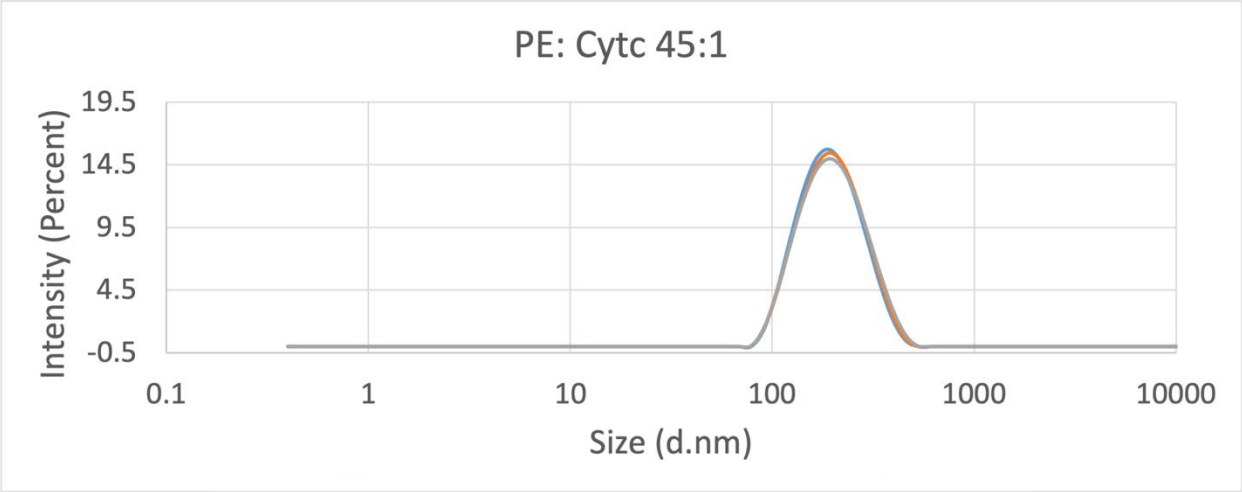

Figure S39: Size Distribution by Intensity for PE: Cytc 45:1 nanoparticle solution after centrifugation and extrusion

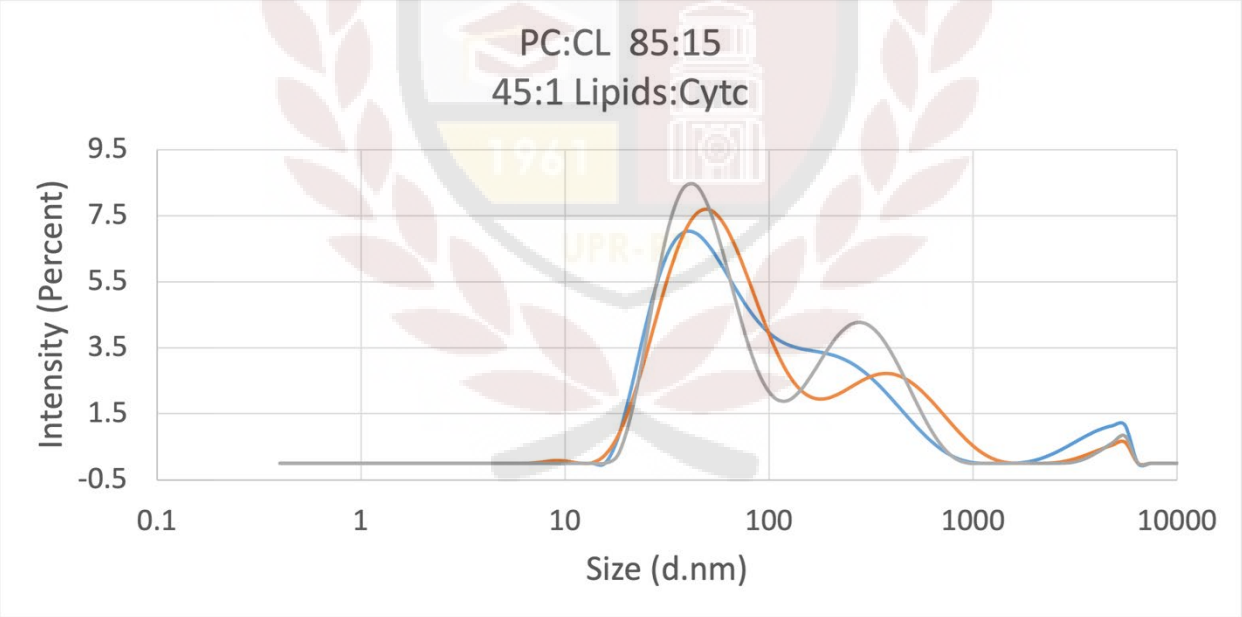

Figure S40: Size Distribution by Intensity for 45:1 Lipids (85:15 PC: CL): Cytc nanoparticle solution after extrusion

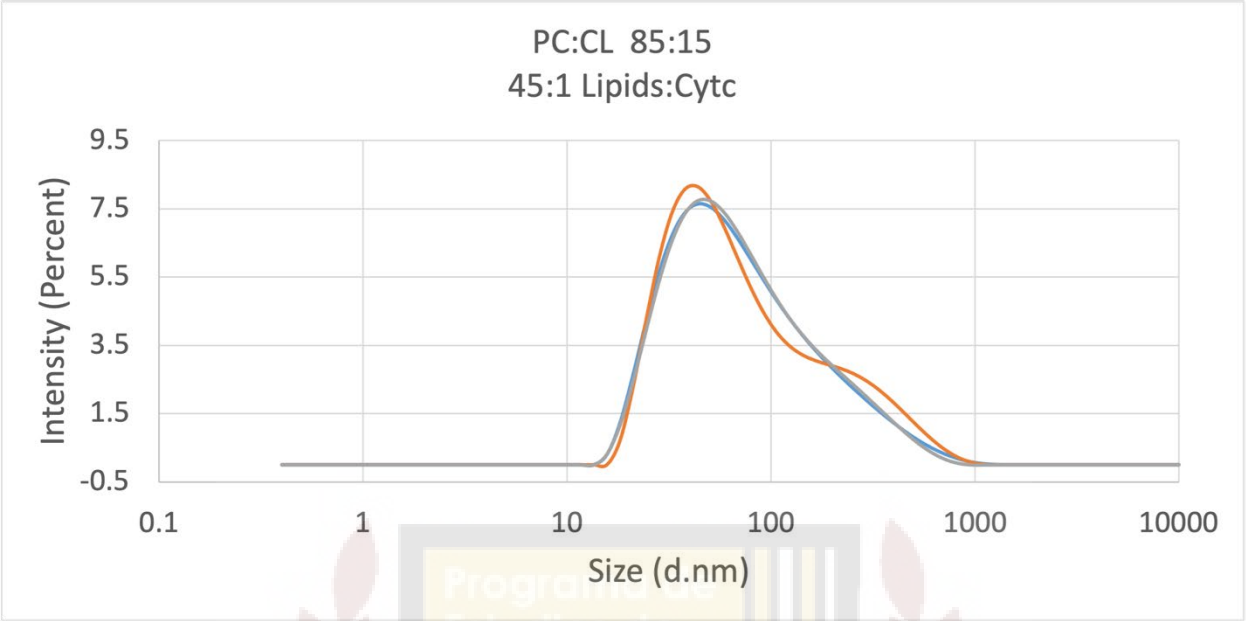

Figure 41: Size Distribution by Intensity for 45:1 Lipids (85:15 PC: CL): Cytc nanoparticle solution after centrifugation and extrusion

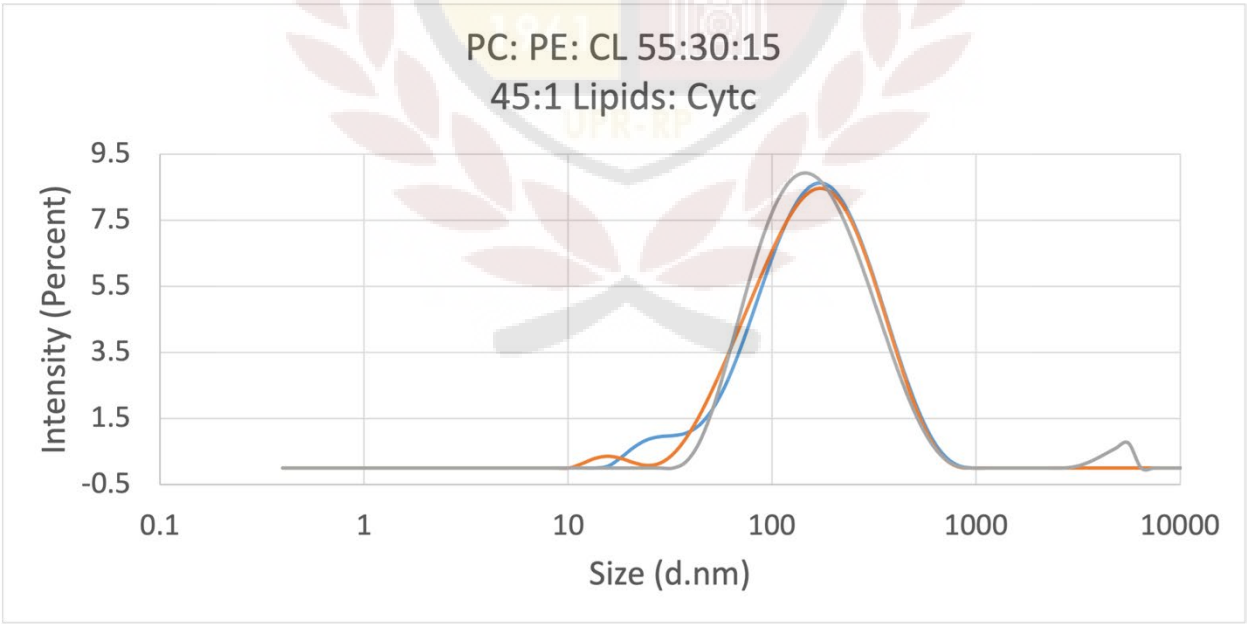

Figure S42: Size Distribution by Intensity for 45:1 Lipids (55:30:15 PC: PE: CL): Cytc nanoparticle solution after extrusion

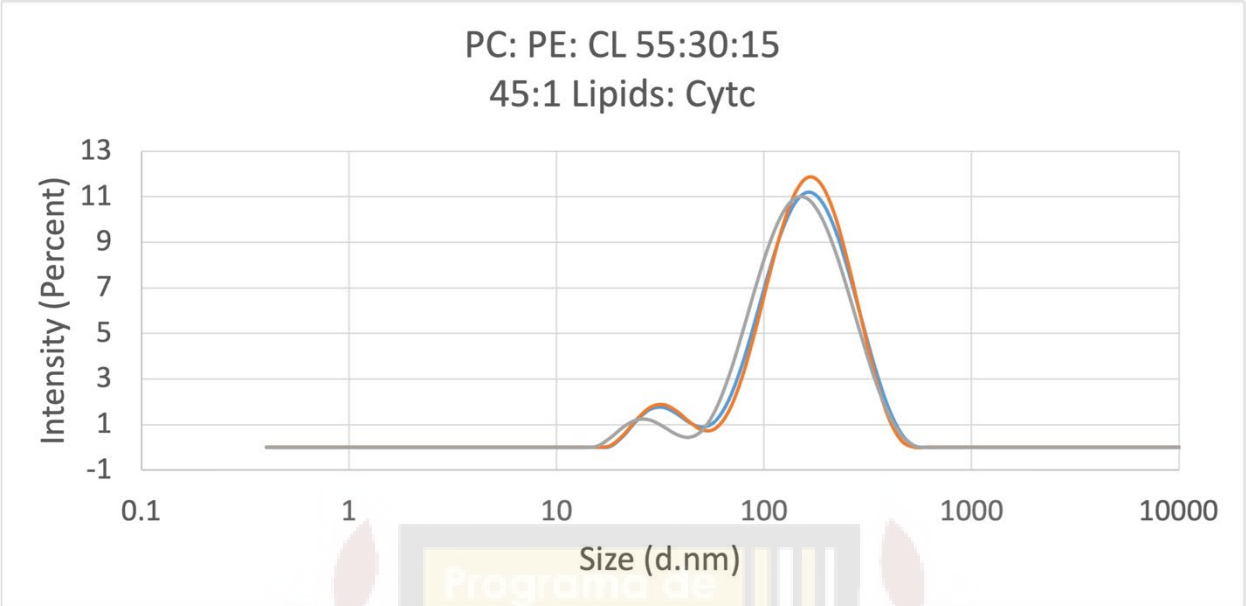

Figure S43: Size Distribution by Intensity for 45:1 Lipids (55:30:15 PC: PE: CL): Cytc nanoparticle solution after centrifugation and extrusion